

**EFFECT OF ENDOGENOUS AND EXOGENOUS
AGENTS IN PLATELET ADHESION**

by

Sowjanya Dokku, B.Tech., M. Tech.

A Dissertation Presented in Partial Fulfillment
of the Requirements of the Degree
Doctor of Philosophy

COLLEGE OF ENGINEERING AND SCIENCE
LOUISIANA TECH UNIVERSITY

February 2022

LOUISIANA TECH UNIVERSITY

GRADUATE SCHOOL

December 17, 2021

Date of dissertation defense

We hereby recommend that the dissertation prepared by

Sowjanya Dokku, B.Tech., M.Tech.

entitled **Effect of Endogenous and Exogenous Agents in Platelet Adhesion**

be accepted in partial fulfillment of the requirements for the degree of

Doctor of Philosophy in Biomedical Engineering



Steven A. Jones

Supervisor of Dissertation Research



Steven A. Jones

Head of Biomedical Engineering

Doctoral Committee Members:

Bryant C. Hollins

Gergana G. Nestorova

Sven Eklund

Teresa A. Murray

Approved:



Hisham Hegab

Dean of Engineering & Science

Approved:



Ramu Ramachandran

Dean of the Graduate School

ABSTRACT

Platelet adhesion is regulated by both activators, such as adenosine diphosphate, and inhibitors, such as nitric oxide (NO). Both agents are released on platelet activation, so that platelets initiate both positive and negative feedback systems. In vivo platelet adhesion models generally consider the effects of platelet activators and inhibitors separately. The goal of this study was to create an environment in which interplay between positive and negative feedback can be observed together and in which the roles of endogenous and exogenous platelet activators are distinguishable. The results are expected to be applicable to the design of stents, which are susceptible to thrombus formation, and which provide multiple adjacent regions where platelet-released agents can interact with one another.

To distinguish between the role of exogenous and endogenous agents, microchannels were produced that had multiple thrombogenic (fibrinogen) regions separated by non-thrombogenic (BSA-coated) regions. This geometry reveals the effect of agents released from different thrombogenic regions on one another. Adhesion was quantified by percent platelet surface area coverage.

Surface area coverage differed between the upstream and downstream sides of the thrombogenic regions. Positive and negative feedback effects were enhanced by increased platelet production of activator and inhibitor. In contrast, when the NO donor

DPTA NONOate was added, with the intent to overwhelm the endogenous feedback, a more uniform spatial distribution of adhesion was obtained.

Though these agonists, activator (ADP) and inhibitor (NO), act on different receptors through different signaling pathways, they all lead to increase or decrease in the intracellular Ca^{2+} concentration ($[\text{Ca}^{2+}]$) depending on the agonist produced. Ca^{2+} is a key component and serves as second messenger in all cells regulatory processes. The increase in $[\text{Ca}^{2+}]$ leads to several steps of activation. The process leading Ca^{2+} to increase and decrease and its underlying mechanisms remained largely unknown.

To examine Ca^{2+} response, platelets were loaded with the Fluo-4 Ca^{2+} ion indicators and fluorescence waveform was monitored. We found that Ca^{2+} response increased dose dependently with addition of an activator (ADP) and addition of endogenous (L-Arginine) and exogenous (DPTA NONOate) NO donor showed decrease in Ca^{2+} response in ADP stimulated platelets.

APPROVAL FOR SCHOLARLY DISSEMINATION

The author grants to the Prescott Memorial Library of Louisiana Tech University the right to reproduce, by appropriate methods, upon request, any or all portions of this Dissertation. It is understood that “proper request” consists of the agreement, on the part of the requesting party, that said reproduction is for his personal use and that subsequent reproduction will not occur without written approval of the author of this Dissertation. Further, any portions of the Dissertation used in books, papers, and other works must be appropriately referenced to this Dissertation.

Finally, the author of this Dissertation reserves the right to publish freely, in the literature, at any time, any or all portions of this Dissertation.

Author _____

Date _____

DEDICATION

This dissertation is dedicated to the memory of my beloved Grandparents, Kolusu Bairagi, Kolusu Venkateswaramma, Dokku Naraiah, and Dokku Chandramathi. A special feeling of gratitude to my loving parents, Venkateswar Rao Dokku and Bharathi Kumari Dokku whose words of encouragement and push for tenacity ring in my ears. It is because of my husband, Shashikanth Chennu, and his 100% confidence in my ability strived me to reach new heights. My sister, Naga Lakshmi Dokku, my brother, Nagendra Babu Dokku and my brother-in-law Sreenivasa Rao Sanakam have never left my side and are very special. My maternal uncles Narasimha Rao and Siva Ram Krishna Kolusu, thank you for believing in me from the time I was young; you have been my backbone of encouragement that has pushed me to the finish line. To my in-laws, Anantharam and Swaroopa Chennu, this would not have been possible without your time, help, and support. It is because of all of you that I have had opportunity to accomplish something that few people have.

TABLE OF CONTENTS

ABSTRACT.....	iii
APPROVAL FOR SCHOLARLY DISSEMINATION	v
DEDICATION	vi
LIST OF FIGURES	xi
LIST OF TABLES	xv
ACKNOWLEDGMENTS	xvi
CHAPTER 1 INTRODUCTION	1
1.1 Cardiovascular Diseases and Atherosclerosis.....	1
1.2 Positive and Negative Feedback Effects on Thrombus Formation.....	2
1.3 Endogenous Platelet Activators and Inhibitors.....	3
1.4 NO and NO Donors	4
1.5 Calcium Signaling in Platelets.....	5
1.6 Role of Calcium in Platelet Activating and Inhibiting Pathways	6
1.7 Analysis of Need.....	8
1.8 Hypotheses.....	10
1.9 Objectives	12
CHAPTER 2 BACKGROUND	13
2.1 Platelet Physiology	13
2.2 Thrombogenic and Non-thrombogenic Regions.....	14
2.3 Fibrinogen.....	15
2.4 DPTA NONOate.....	16

2.5	Shear Rates	17
2.6	Devices for the Study of Platelet Adhesion	18
CHAPTER 3 METHODS		21
3.1	Experimental Process for Microchannels	21
3.2	Chemicals Used for Both the Protocols	22
3.2.1	Chemical Preparation	22
3.2.2	Bovine Blood Source	24
3.2.3	Preparation of PRP	24
3.2.4	CFSE-Labelled PRP	24
3.2.5	Preparation of Microchannels	25
3.2.6	Silane Slide Preparation	26
3.2.7	Quartz Glass Slide Preparation	27
3.2.8	Microchannel Fabrication	27
3.3	Perfusion of PRP Through the Channels	27
3.4	Mathematical Modeling of PRP Flow in Micro Channels	28
3.5	Addition of Activators and Inhibitors	29
3.5.1	Effects of ADP and NO on Platelets	29
3.6	Syringe Filling	30
3.7	Calculation of NO Concentration from an NO Donor	32
3.8	Fluorescent Microscopy	32
3.9	Experimental Process for Calcium Imaging	33
3.9.1	Chemicals Used in Calcium Signaling in Platelets	34
3.9.2	Platelet Extraction	34
3.9.3	Treating Platelets with Calcium Ion Indicators	34
3.9.4	Calcium Activity in Platelets with Platelet Activators and Inhibitors.	35

3.9.5	Calcium Imaging After Treatment with Chemical Agents	35
3.9.6	Measuring and Analyzing Calcium Fluorescence Intensity	36
3.10	Statistical Analysis.....	36
CHAPTER 4 RESULTS		38
4.1	Platelet Surface Area Coverage	38
4.2	Experiment Controls	41
4.3	Effect of ADP Concentrations on Platelet Surface Area Coverage.....	42
4.3.1	Statistics	46
4.4	Effect of L-Arginine on PSAC	47
4.4.1	Statistics	50
4.5	Effect of DPTA NONOate on PSAC.....	51
4.5.1	Statistics	54
4.6	Combined effect of ADP and LA on PSAC	55
4.6.1	Statistics	57
4.7	Combined Effect of ADP- DPTA NONOate on PSAC.....	58
4.7.1	Statistics	60
4.8	Calcium Activity in Platelets	61
4.8.1	Effect of ADP on Calcium Activity in Platelets.....	61
4.8.2	Combined Effect of ADP and L-Arginine on Calcium Activity in Platelets	64
4.8.3	Effect of ADP-DPTA NONOate on Calcium Activity.....	67
CHAPTER 5 DISCUSSION.....		71
5.1	Effect of ADP Concentrations on PSAC	72
5.2	Effect of L-Arginine on PSAC	73
5.3	Effect of DPTA NONOate on PSAC.....	74
5.4	Combined Effect of ADP with Exogenous and Endogenous NO donors on PSAC	75

5.4.1	Combined Effect of ADP-L-A on PSAC.....	75
5.4.2	Combined Effect of ADP- DPTA NONOate on PSAC.....	76
5.5	Effect of ADP, L-A, and DPTA NONOate on Calcium Signaling	77
5.6	Effects of Shear Rates.....	78
5.7	Comparison of Results to Other Sources	79
5.8	Sources of Experimental Errors	82
5.9	Variability in Experiments.....	83
CHAPTER 6 CONCLUSIONS AND FUTURE WORK.....		85
6.1	Conclusions.....	85
6.2	Future Work.....	86
6.2.1	Platelets Count	86
6.2.2	Patterning of Proteins Using Nano eNabler.....	86
6.2.3	Effect of Proteins on Platelet Adhesion	87
6.2.4	Real-Time Analysis	87
6.2.5	Combined Effect of ADP- DPTA NONOate on PSAC.....	87
6.3	Future Applications.....	87
APPENDIX A PROGRAM USED TO CALCULATE PSAC.....		89
BIBLIOGRAPHY.....		92

LIST OF FIGURES

Figure 1-1: The mechanism leading to thrombus formation [8].....	2
Figure 1-2: Pathway leading to NO from L-Arginine to L-citrulline through the reaction catalyzed by NOS enzyme [18].	4
Figure 1-3: Mechanism of NO Inhibition [8].	5
Figure 1-4: Ca ²⁺ signaling in ADP-induced platelet activation and aggregation [31].....	7
Figure 1-5: Endogenous and Exogenous NO signaling in Platelets [32]	8
Figure 3-1: Experimental set up for the microchannel flow system.....	22
Figure 3-2: The microchannel with inlet and outlet flow units.....	25
Figure 3-3: Slide with the pre-cut Kapton tape pattern.....	26
Figure 3-4: Silane Slide patterned with thrombogenic region (green) and non-thrombogenic region (gray).	27
Figure 3-5: Flow between two fixed parallel plates.....	28
Figure 3-6: Nomenclature for the images taken from the slide.	33
Figure 4-1: Overall adhesion of platelets from upstream to downstream regions of the microchannel.....	38
Figure 4-2: Image A is first image of region T1 from the base slide perfused with CFSE labeled platelets with no chemical at a shear rate of 1500 s ⁻¹ . A) Original image, B) Binary Image.....	39
Figure 4-3: Sample Image from the base slides, with no chemical added, perfused with CFSE labeled platelets at a shear rate of 1500 s ⁻¹ . Overall average percent surface coverage is 62.2. A) Unprocessed image B) Binary of Image A.	39
Figure 4-4: Image from the base slides, with no chemical added, perfused with CSFE labeled platelets at a shear rate of 1500 s ⁻¹ . Overall average percent surface coverage is 93.0 A) Original image, B) Binary of Image A.	40

Figure 4-5: Slide imaged in FITC after addition of the fibrinogen. The tagged fibrinogen (green) is to the left, and the blocked BSA (black) region is to the right for both image A (Region covering NT1 and T2) and image B (region covering NT2 and T3).....	40
Figure 4-6: Images of the fibrinogen regions at each step of the experimental process. Image A: blank slide. Image B: after addition of BSA. Image C: after addition of untagged fibrinogen. Image D: after perfusion with unlabeled PRP.....	41
Figure 4-7: Control images of non-thrombogenic regions after perfusion of channels with CFSE labelled platelets, as recorded from four different experiments. Image A: No Chemical Added, Image B: ADP added, Image C: L A added, Image D: DPTA NONOate.	42
Figure 4-8: Sample images from non-thrombogenic regions (Images A & B are from NT1; Images C and D from NT2) when fibrinogen is outside of the marked region.....	42
Figure 4-9: Platelet adhesion under different concentrations of ADP 0, 2, 5 and, 10 $\mu\text{M/L}$ in first, second, third and, fourth row, respectively. Images T1, NT1, T2, NT2, and T3 in each row represents nomenclature for the images taken from the slide as mentioned in Figure 4-1 and Figure 3-6.	44
Figure 4-10: Experimental results on overall percent surface area coverage with no chemical, 2 $\mu\text{M/L}$ ADP, 5 $\mu\text{M/L}$ ADP, 10 $\mu\text{M/L}$ ADP added perfused at a shear rate of 1500 s^{-1} . Error bars represent standard deviation.	45
Figure 4-11: Experimental results on effect of percent surface area coverage for different concentration of ADP on microchannel from upstream to downstream say T1-NT1-T2-NT2. Error bars represent standard deviation.....	46
Figure 4-12: Platelet adhesion under different concentrations of L-A 5,10 and, 15 $\mu\text{M/L}$ in first, second, third and, fourth row, respectively. Images T1, NT1, T2, NT2, and T3 in each row represents nomenclature for the images taken from the slide as mentioned in Figure 4-1 and Figure 3-6.	48
Figure 4-13: Experimental results on overall percent surface area coverage with 0, 5, 10, and 15 μM L-A added at a shear rate of 1500 s^{-1} . Error bars represent standard deviation.....	49
Figure 4-14: Experimental results on effect of percent surface area coverage for different concentration of L-A on microchannel from upstream to downstream say T1-NT1-T2-NT2. Error bars represent standard deviation.....	50
Figure 4-15: Platelet adhesion under different concentrations of DPTA NONOate 0, 5,10 and, 15 $\mu\text{M/L}$ in first, second, third row, and fourth row respectively. Images T1, NT1, T2, NT2, and T3 in each row represents nomenclature for the images taken from the slide as mentioned in Figure 4-1 and Figure 3-6.....	52

- Figure 4-16:** Experimental results on overall percent surface area coverage with 0, 5, 10, 15 $\mu\text{M/L}$ DPTA NONOate added to the PRP, which was then perfused at a shear rate of 1500 s^{-1} . Error bars represent standard deviation. 53
- Figure 4-17:** Experimental results on effect of percent surface area coverage for different concentration of DPTA NONOate on microchannel from upstream to downstream say T1-NT1-T2-NT2. Error bars represent standard deviation. 54
- Figure 4-18:** Overall platelet adhesion of platelets for all combination of different concentrations of ADP and L-Arginine. 56
- Figure 4-19:** Experimental results on effect of percent surface area coverage on combined effect of ADP and LA for different combinations concentrations on microchannel from upstream to downstream say T1-NT1-T2-NT2. Error bars represent standard deviation. 57
- Figure 4-20:** Overall platelet adhesion of platelets for all combination of different concentrations of ADP and DPTA NONOate. 59
- Figure 4-21:** Experimental results on effect of percent surface area coverage on combined effect of ADP and DPTA NONOate for different combinations concentrations on microchannel from upstream to downstream say T1-NT1-T2-NT2. Error bars represent standard deviation. 60
- Figure 4-22:** Calcium activity in platelets treated with activating stimulus (A) before stimulation (control), (B) after ADP stimulation, and (C) after ionomycin stimulation (positive control). 62
- Figure 4-23:** Calcium signals recorded for platelets when stimulated with agonists ADP 0,2,5, and $10\mu\text{M}$ concentrations. The X-axis represents frame number and 1 frame = 4 seconds, Y-axis represents normalized fluorescent intensity values. 63
- Figure 4-24:** Graph showing the peak of the calcium response in platelets stimulated with ADP. Each bar is the averages of $N=3$ experiments with two wells per condition, and with the number of samples (cells) ranging from $n=20$ to 120. Error bars represent standard deviation values. 64
- Figure 4-25:** Calcium signals recorded for the ADP of $12.5 \mu\text{M}$ stimulated platelets with the addition of L-A $12.5 \mu\text{M}$. The X-axis represents frame number and 1 frame = 4 seconds, Y-axis represents normalized fluorescent intensity values. 66
- Figure 4-26:** Graph showing results for peak calcium response after L-A is added to platelets stimulated with ADP to the normalized fluorescence intensities. Data represent the averages of $N=3$ experiments with two wells per condition, and no. of samples (cells) ranging from $n= 20$ to 120. Error bars represent standard deviation values. 67

Figure 4-27: Calcium signals recorded when DPTA NONOate is added to ADP-stimulated platelets. The X-axis represents frame number and 1 frame = 4 seconds, Y-axis represents normalized fluorescent intensity values. 69

Figure 4-28: Peak calcium response of DPTA NONOate on platelets stimulated with ADP to the normalized fluorescence intensities. Data represent the averages of N=3 experiments with two wells per condition, and no. of samples (cells) ranging from n= 20 to 120. Error bars represent standard deviation values. 70

LIST OF TABLES

Table 3-1: Summary of Parameters used in experiments.....	31
--	----

ACKNOWLEDGMENTS

I would like to extend my sincere gratitude and thanks to my advisor Dr. Steven Jones for all his assistance and guidance throughout the duration of this research. I feel extremely fortunate to have been able to work with such a talented, and outstanding individual.

I must acknowledge the people that have contributed to my success in completion of this work. I thank Dr. Sreenivasa Rao Sanakam and Dr. Regina Roney Adams for their advice and willingness to talk through issues and share their knowledge and experience helped my dissertation tremendously. The knowledge shared by Dr. DeCoster strongly affected this research. Dr. Neela Prajapati and Dr. Kevin Holly's for their valuable suggestions and help when in need. My research would not have been possible without their help. Dr. Hollins and Dr. Crews gave the knowledge to help get through some of the toughest issues, which is greatly appreciated. I would like to thank all my committee members, for offering valuable suggestions and feedback.

I would also like to thank the College of Engineering and Science (COES) and the Center for Biomedical Engineering and Rehabilitation Science (CBERS) for allowing me to pursue my dream. Special thanks go to Gorden and Benny from tech farm for all their assistance through the years.

I would also like to thank my parents, my elder sister, my brother-in-law, in-laws and all my cousins. They were always supporting me and encouraging me with their best

wishes. Lastly, I would like to thank my husband for his unwavering support and encouragement during all my good and bad times.

CHAPTER 1

INTRODUCTION

1.1 Cardiovascular Diseases and Atherosclerosis

The main cause of cardiovascular disease (CVD), including myocardial infarction (MI), heart failure, stroke, and claudication, is atherosclerosis [1]. This condition affects about one-third of all deaths in people older than 35 years every year, and the percentage is expected to continue increasing in developing countries in coming years [2].

Atherosclerosis involves lipid and macrophage accumulation inside the lumen of large arteries. Atherosclerotic plaque disruption leads to platelet activation, platelet aggregation, and consequent atherothrombotic episodes [3]. **Figure 1-1** illustrates the development and progression of atherosclerosis and thrombosis through platelet activation and aggregation [4].

Atherosclerosis plaque ruptures cause thrombus formation, which triggers cardiovascular diseases [5][6]. It is generally not localized to one region or one lesion, but is more irregular and frequently diffuse, forming multiple thrombi that alter hemodynamics of the system. Platelet physiology and its functions play a key role in initiation and progression of atherosclerotic lesions through release of chemical agents, granule proteins, and micro particles by interacting with low density lipid proteins, immune cells, and endothelial cells [7]. Thus, effective primary prevention strategies and tools that can identify risk groups are needed worldwide. Models that elucidate dynamic

changes and early prediction of blockages in blood vessels can assist in the development of these needs.

1.2 Positive and Negative Feedback Effects on Thrombus Formation

The atherosclerotic plaque rupture by platelets is a pathological stimulus for thrombus formation. Thrombus formation alone has both spatial and temporal features embraced with diverse biochemical, biomechanical, and biophysical interactions. **Figure 1-1** summarizes the events leading to the formation of a thrombus [8].

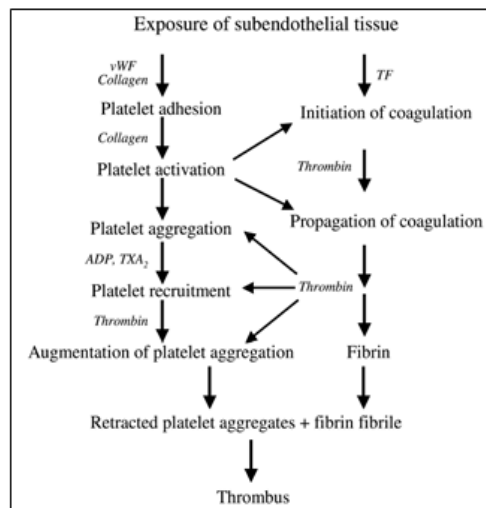


Figure 1-1: The mechanism leading to thrombus formation [8].

The complexity of the process increases when multiple thrombi interact spatially and temporally. Platelet-to-platelet signaling is expected to have both positive and negative feedback effects on thrombus formation [9]. Generally positive feedback leads to rapid responses and must be regulated by negative feedback to stop unbounded growth and oscillatory behavior.

Platelets generally experience numerous extracellular signals at same time and respond to a complex combination of primary and secondary activator signals in addition

to opposing inhibitory signals. The interaction is regulated such that each response triggered by a single agonist. But a more sophisticated approach is needed to incorporate multiple agonists and pathways, which themselves interact into a signaling network. When blood interacts with a series of activators from the vessel wall (positive feedback) and inhibitors (negative feedback), the combined effect of activating and inhibiting network led to many complications related to platelets [10][11].

1.3 Endogenous Platelet Activators and Inhibitors

Platelet activation, aggregation, and adhesion depend on exogenous and endogenous activators and inhibitors [12]. The interaction between inhibitors such as nitric oxide (NO) and activators such as adenosine diphosphate (ADP) depends on the temporal sequence of release of these agents [13][14]. The positive feedback, originating in endogenous agents that recruit and activate additional platelets, leads to regions of rapid thrombus growth, but endogenous negative feedback compounds can inhibit this growth. Consequently, the overall growth of a downstream thrombus will be changed by an upstream thrombus in a manner that depends on whether the activators or the inhibitors from the upstream thrombus are more dominant and cannot be predicted.

A method to study the effects of spatial relationships on platelet adhesion is to develop a model that includes platelet adhesion at the site of interfaces between activating region and non-activating regions on the flow surface, such a model can elucidate the relative effects of positive and negative feedback at different regions in the flow. The focus of this dissertation is the activator ADP and inhibitor NO when supplied exogenously in various ratios or triggered endogenously.

1.4 NO and NO Donors

The most important known endogenous vasodilator secreted by vascular endothelium is NO [15]. NO is produced within platelets by enzyme NO synthase (eNOS) and effectively inhibits platelet adhesion and aggregation [16]–[18]. It is formed by a twostep oxidation process of L-Arginine (a semi essential amino acid) to L-citrulline, as shown in **Figure 1-2**. It is a byproduct of this conversion, which involves Nicotinamide Adenine Dinucleotide Phosphate (NAPDH) and oxygen, with the intermediate NG-hydroxy-L-Arginine [19].

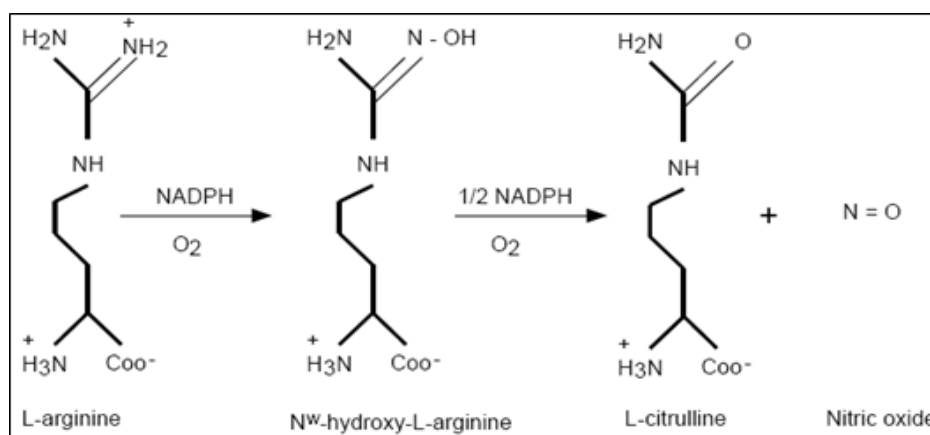


Figure 1-2: Pathway leading to NO from L-Arginine to L-citrulline through the reaction catalyzed by NOS enzyme [20].

It inhibits platelet activation by increasing cyclic-3'5'-guanosine monophosphate (cGMP) with direct stimulus of the enzyme soluble guanylate cyclase (sGC) [18][21]. sGC stimulates the formation of cyclic GMP from GTP. cGMP activates protein kinase G (PKG) which blocks Phospholipase C which in turn blocks inositol triphosphate (IP₃) receptors. **Figure 1-3** diagrams the mechanism of NO and platelet inhibition.

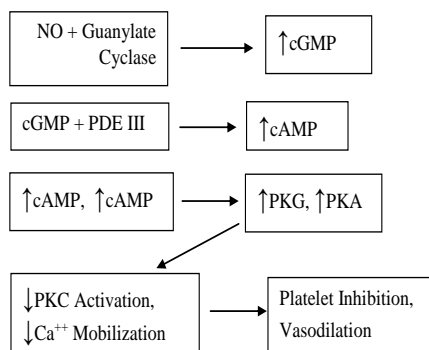


Figure 1-3: Mechanism of NO Inhibition [8].

NO production by platelets is low in patients with cardiovascular risk factors, heart disorders, and coronary heart disease, and in some situations, it also leads to arterial thrombotic disease [22][23]. Excessive production of NO by iNOS also leads to many harmful effects such as inflammation and initiation of apoptosis [24]. Thus, exogenous NO donors, which are pharmacological compounds that release NO instantly, are used widely in cardiovascular physiology and therapeutics to evaluate the role of NO in platelet Ca^{2+} signaling and its functions [25][26].

The replacement of endogenous NO by exogenous NO donors like Dipropylentriamine NONOate (DPTA NONOate) in platelet pathobiology has become great foundation in the field of cardiovascular medicine [27]. Our aim is to study how exogenous NO donors modulate the bioactivity of endogenously produced NO on ADP stimulated platelets.

1.5 Calcium Signaling in Platelets

Platelets are activated through many signaling pathways. Various agonists bind to specific receptors to trigger platelet function in a dose-dependent manner. Platelets respond to collagen, ADP released from activated platelets, thromboxane, and thrombin while simultaneously being modulated by NO and prostacyclin [28]. These chemical

agents either increase or decrease intracellular Ca^{2+} concentration ($[\text{Ca}^{2+}]$) depending on the agonist produced, though they act on different receptors through different signaling pathways. Ca^{2+} is a key component that serves as second messenger in all cells regulatory processes. The increase in $[\text{Ca}^{2+}]$ leads to several steps of activation [29][30]. The process leads Ca^{2+} to increase and decrease, and its underlying mechanisms remain largely unknown. The major Ca^{2+} sources for platelet activation and inhibition are not fully identified. Platelet activation models generally consider the effects of platelet activators and inhibitors separately. This study was undertaken to determine the interaction between positive and negative feedback effects produced by an activator (ADP) and an inhibitor (NO), as measured by the effect on $[\text{Ca}^{2+}]$.

1.6 Role of Calcium in Platelet Activating and Inhibiting Pathways

Ca^{2+} is an essential second messenger and a highly versatile intracellular signal that process over a wide range of platelet functions. Ca^{2+} signaling uses an ‘ON’ reaction that introduces Ca^{2+} into the cell and an ‘OFF’ reaction that removes it from the cytoplasm. Channels in plasma membrane and endoplasmic/sarcoplasmic reticulum are responsible for ON reactions whereas pumps and exchangers carry out OFF reactions. The agonists act through two classes of signaling receptors, which are immuno receptor tyrosine-based activation motif (ITAM-Coupled) receptors and G protein-coupled receptors (GPCR). These receptors trigger different signaling pathways and activate phospholipase (PLC) isoforms. PLC isoforms produce diacylglycerol (DAG) and IP3 (Inositol triphosphate receptors) thereby inducing the release of Ca^{2+} from dense tubular systems in endoplasmic reticulum. This store depletion triggers a large Ca^{2+} influx across the cytosol called store operated Ca^{2+} entry (SOCE), which is major route of Ca^{2+} influx

in platelets. **Figure 1-4** illustrates the Ca^{2+} signaling in ADP-induced platelet activation [31].

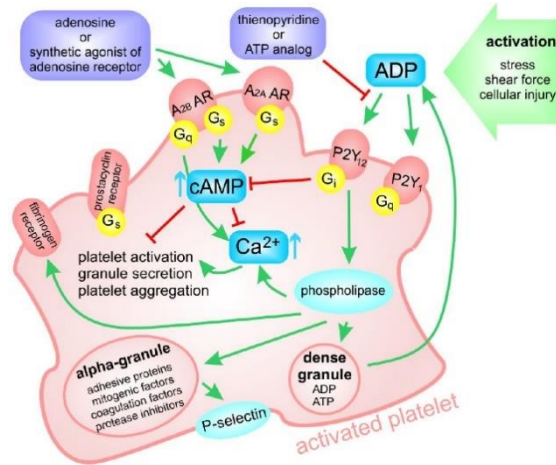


Figure 1-4: Ca^{2+} signaling in ADP-induced platelet activation and aggregation [31].

Endothelial cells inhibit platelet inhibition through production of NO by the enzyme endothelial NOS (eNOS). NOS is strictly a Ca^{2+} /CaM dependent enzyme which enters platelets and activate enzyme sGC, which then stimulates the formation of cyclic GMP from GTP. CGMP activates PKG, which blocks phospholipase C, which in turn blocks IP3 and decreases the intracellular calcium concentrations. Exogenous donors such as DPTA NONOate are converted to NO and could replace deficient levels of NO in patients with coronary artery disease (CAD).

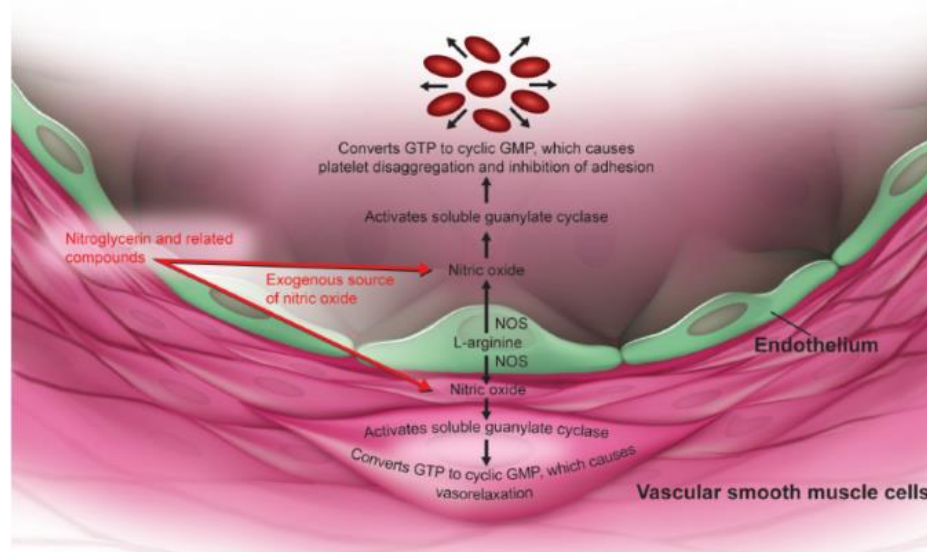


Figure 1-5: Endogenous and Exogenous NO signaling in Platelets [32].

Figure 1-5 illustrates the process; NO release from endothelial cells activates soluble guanylate cyclase with increases the level of intracellular cyclic guanosine monophosphate (cGMP) and thus causing vasorelaxation, platelet disaggregation, and prevention of platelet adhesion by inhibiting the $[Ca^{2+}]$ levels in platelets [32].

Replacement with exogenous NO donors is helpful in patients with the impaired activity of the endothelial L-Arginine/NO pathway.

1.7 Analysis of Need

Many models are being developed for platelet-mediated thrombo-genesis, but these models separately consider the effects of platelet activators and inhibitors. Combined effects of positive and negative feedback signals acting at various locations are the main controlling factors of the final thrombus size. To explain these effects, positive and negative feedback effects need to be studied simultaneously on regions in which thrombus formation is active next to regions in which thrombus is prevented. This configuration allows examining the effects of platelet derived activators and inhibitors in

one region influences platelets in a different region under varying shear conditions. This type of study requires spatially varying proteins surfaces coated with proteins. The limited knowledge about the relation between platelet function and the adhesion patterns that would occur made us to propose a model which examines and compare platelet adhesion and its combined effects on positive and negative feedback interactions on an improved micro channel patterned with fibrinogen using Xurography. The experiments done are an extension of the work done by Sanakam, and Adams. Sanakam and Adams built a micro channel patterned with thrombogenic regions and non-thrombogenic region (one that has thrombogenic and non-thrombogenic surfaces side-by-side) to study simultaneous positive and negative feedback effects on regions in which thrombus formation is active next to regions in which thrombus is prevented. Their results suggest an influence of agents secreted by upstream platelets on downstream adhesion, but some of the results were not statistically significant, and there is need to collect enough data to be able to quantitatively model the effects [33][34]. Combined positive and negative feedback signals acting at various locations are the main controlling factors of the final thrombus size.

Sanakam and Adams did not concentrate on the combined effects of chemical agents and did not study the percent surface area coverage and its effects when production of NO is prevented with the addition of L-NMMA or ADP to the plasma along a thrombogenic surfaces. These endogenous agents will be used to test various strategies to inhibit thrombus formation under flow conditions and to minimize the impact on hemostasis.

Sanakam and Adams also did not study exogenous NO donors. A Xurography

technique was used to layer each micro channel with collagen or fibrinogen or albumin and compared the percentage of platelets covered on the surface area. Platelets were extracted from bovine whole blood and will be labeled with CFSE and enriched with L-Arginine (L-A), ADP, and/or N^G-Methyl-L-Arginine acetate salt (L-NMMA) and NO donors like DPTA-NONOate. CFSE-labeled platelet-rich plasma (PRP) was perfused through the micro channel under varying conditions. Micro channels were then imaged using a fluorescence microscope and then processed with a MATLAB program to determine percent surface area coverage.

Platelet agonists release Ca²⁺ from intracellular stores during platelet activation plays a crucial role in regulating many platelet functions. Activation and inhibition pathways of platelets trigger calcium stores in platelets [28][35]. eNOS-produced NO requires Ca²⁺ entry for prolonged activation [36]. The process leading Ca²⁺ to increase and decrease and its underlying mechanisms remain largely unknown, and the major Ca²⁺ sources for platelet activation and inhibition are not fully identified. To examine Ca²⁺ flux, platelets were loaded with the Fluo-4 Ca²⁺ ion indicators and fluorescence waveform was monitored. Thus, our aim is to measure the elevations in [Ca²⁺] with addition of exogenous and endogenous chemical agents to platelets loaded with Fluo-4 Ca²⁺ ion indicators where fluorescence waveform was monitored.

Therefore, the following hypotheses and specific aims have been generated to fulfill this need.

1.8 Hypotheses

The hypotheses of this study are:

Hypothesis 1: Percent surface area coverage of platelets will increase dose-dependently when platelet derived activators (e.g., ADP) are included in the perfused plasma but will be different on the upstream and downstream sides of thrombogenic surface.

Hypothesis 2: Percent surface area coverage of platelets will decrease dose-dependently when NO substrate L-Arginine is added endogenously to the perfused plasma but will differ on the upstream and downstream sides of thrombogenic surface.

Hypothesis 3: Percent surface area coverage of platelets will decrease dose-dependently when exogenous NO donor DPTA NONOate is added, as inhibitor, to the perfused plasma but will differ on the upstream and downstream sides of thrombogenic surface.

Hypothesis 4: Percent surface area coverage of platelets will increase for a given plasma L-Arginine concentration as plasma ADP concentration increased. Likewise, when for a given ADP concentration, platelet surface area coverage will decrease as L-Arginine concentration increases and will differ on the upstream and downstream sides of thrombogenic surface.

Hypothesis 5: For a given amount of DPTA NONOate added to the PRP, platelet surface area coverage will increase with increased plasma ADP concentration. Likewise, for a given amount of ADP added to the plasma, platelet surface area coverage will decrease and will differ on the upstream and downstream sides of thrombogenic surface.

Hypothesis 6: Plasma free platelets loaded with fluorescent Ca^{2+} indicators Fluo-4 will induce a dose-dependent rise in $[\text{Ca}^{2+}]$ with addition of an activator, ADP indicating platelet activation through calcium signaling.

Hypothesis 7: Addition of LA will decrease Ca^{2+} peaks, demonstrating the immediate inhibition effect of NO synthase endogenously in ADP stimulated platelets.

Hypothesis 8: Addition of exogenous NO donor DPTA NONOate, with the intent to overwhelm the endogenous feedback through platelet NO production, will decrease $[\text{Ca}^{2+}]$ peaks.

1.9 Objectives

These hypotheses will be tested with the following methods:

1. A micro channel system will be created in which each channel is coated with three isolated patches of fibrinogen, through a Xurography technique in such a way that the channels can be exposed to flowing PRP under controlled shear stresses.
2. In separate experiments, the individual agents ADP, L-Arginine, and DPTA-NONOate will be added to the PRP prior to injection through the channels, and the amount of adhesion will be quantified as a function of the concentration of each agent.
3. Combined concentrations of the three agents will be added to the PRP prior to injection through the channels, and the amount of adhesion will be quantified as a function of the ratios of concentrations of the agents.
4. Performing Calcium signaling experiments with platelet poor plasma loaded with Fluo-4 Ca^{2+} ion indicators where fluorescence waveform was monitored to measure is to measure the elevations in $[\text{Ca}^{2+}]$ with addition of exogenous and endogenous chemical agents to platelets.

CHAPTER 2

BACKGROUND

2.1 Platelet Physiology

Platelets, known as thrombocytes, are small diameter, approximately 1-5 μ m. They are present in larger number, about 150,000 to 400,000 per cubic millimeter of blood, than white blood cells, but they occupy a smaller fraction of volume [37].

Platelets lack nuclei and have complex functions and metabolism. At resting state platelets are irregular disc shaped structured bodies. Upon activation they undergo a morphological changes, to a more spherical in shape with finger like extensions (pseudopodia) [38]. The activated platelets have the increased surface area because of their structure and act as an interconnecting mesh, entrapping fibrin fibers and other platelets, forming a thrombus [39].

Platelets are primarily involved in hemostasis, preventing blood loss after injury, with the formation of blood clots known as coagulation [40]. A platelet plug that clots the blood at the site of injury is formed by an accumulation of the platelets on a fibrin mesh with the help of the adhesive surface proteins on the platelet surface [41]. The complicated wound repair process begins only when bleeding has stopped with clot. Coagulation and wound healing release many factors that increase platelet aggregation, mediate inflammation, and promote blood coagulation [42]. A low platelet count (thrombocytopenia) leads to excessive bleeding and impairment of wound healing.

However, a high platelet count (thrombocytosis) leads to formation of blood clots (thrombosis) which can obstruct blood vessel and result in ischemic tissue damage such as stroke, myocardial infarction, pulmonary embolism.

Platelets are in an inactivation state through normal circulation and become activated at the sites of vascular injury [43]. The formation of blood clots is necessary to save life from excessive bleeding upon injury and at the same time abnormal blood clots formed in arteries can cause death. Thus, platelets play important role in both hemostasis and thrombosis [44]. Platelets, after activation, release prothrombogenic substances that amplify thrombus formation and inhibitory agents that control the extent of thrombus formation. Platelets form a thrombus through adherence and aggregation [45].

2.2 Thrombogenic and Non-thrombogenic Regions

Atherosclerosis is an irregular pattern of platelets adhesion and thrombosis found over the surface of lesions. Atherosclerotic lesion rupture leads to thrombus formation, occlusion of the vessel lumen, and heart attack or stroke [7][46]. One mechanism of sudden cardiac death is a coronary lesion in which plaque ruptures and causes a thrombosis that occludes the vessel lumen [47]. Thrombus formation individually has both spatial and temporal characteristics that consist of dynamic complex and diverse biochemical, biophysical and biomechanical interactions [5]. This complexity increases when multiple thrombi interact spatially and temporally [48]. The presence of functional feedback loops (positive and negative), the variations in spatial and temporal relations in flow, and biochemical reactions that activate and inhibit thrombus formation are challenging to understand and predict [49]. Direct interactions between positive and negative feedback mechanisms have not been extensively studied under flow conditions

and are not tested with anticoagulated blood. It is expected that as platelet adhesion grows locally on one thrombogenic region that is separated from another thrombogenic region by a non-thrombogenic region, the agents secreted by the activated platelets will influence adhesion on other thrombogenic region. Thus, to study such mechanisms, platelet adhesion to thrombogenic regions patterned with different types of adhesive proteins like collagen, fibrinogen, and albumin should be studied under the influence of shear rates. The degree of platelet activation and inhibition by the addition of activators and inhibitors on localized thrombogenic regions is needed.

Combined effects of positive and negative feedback signals acting at various locations are the main controlling factors of the final thrombus size. To well explain these effects, positive and negative feedback effects need to be examined on regions in which thrombus formation is active next to regions in which thrombus is prevented. This configuration allows examining the effects of platelet derived activators and inhibitors in one region influences platelets in a different region under varying shear conditions. This type of study requires spatially varying proteins surfaces coated with different proteins.

2.3 Fibrinogen

Platelet adhesion mechanisms are necessary to regulate the excessive bleeding or reduce the blood loss at the sites of vascular injury and at the areas of circulation with highest shear rates [50]. Platelet adhesion at the site of injury is needed to help thrombus formation both in normal hemostasis and compulsive thrombosis [40]. Fibrinogen and von Willebrand factor(vWF) mediate platelet adhesion. Fibrinogen, which is also called factor I, plays important role in both platelet-surface and platelet-platelet interactions, adhesion, and aggregation by binding to the glycoprotein (GP)IIb-IIIa receptor [40][51].

In normal conditions, inactivated circulating platelets, do not interact with plasma fibrinogen. At the site of vascular injury, platelet binding to vWF and collagen become activated and release different agonists. This process triggers the exposure of the binding site of fibrinogen on platelets, the activation depends on GPIIb/IIIa complex. GPIIb/IIIa binds to fibrinogen, thus linking platelets to one another and to fibrinogen attached to the vessel wall [52]. Fibrinogen is thus an important ligand for platelets adhesion to artificial surfaces. Immobilization of fibrinogen on the surface of microchannels in the microfluidic system helps in adhering inactivated platelets for studying their positive and negative feedback effects on thrombogenic and non-thrombogenic regions.

2.4 DPTA NONOate

Exogenous NO donors are pharmacological compounds that release NO instantly, are used widely in cardiovascular physiology and therapeutics [25][26] to evaluate the role of NO in platelet Ca^{2+} signaling and its functions. DPTA NONOate is the most available exogenous NO donor with high diffusion coefficient of NO and consequence of its small size has a significant role in inhibiting activated platelets. DPTA NONOate are converted to NO and could replace deficient levels of NO in patients with CAD. Replacement with exogenous NO donors is helpful in patients with the impaired activity of the endothelial L-Arginine-NO pathway. DPTA NONOate spontaneously dissociates NO with a half-life of three hours at 37°C and five hours at 22-25°C, Ph 7.4.

The replacement of endogenous NO by exogenous NO donors like DPTA NONOate in platelet pathobiology has become great foundation in the field of cardiovascular medicine [27]. Our aim is to study how exogenous NO donors modulate the bioactivity of endogenously produced NO in platelets.

2.5 Shear Rates

Hemodynamic shear forces have been reported to exert direct and indirect effects on platelet reactivity. Shear forces activate platelets leading to spontaneous or facilitated aggregation *in vitro* and stimulate the production of endothelium-derived anti-aggregatory agents. Experiments done in our lab previously by Adams and Sanakam have shown that shear rate affects the degree of adhesion and aggregation of platelets in microchannels [33][34]. A microfluidic system was constructed to simulate the flow of blood near the vessel wall, including shear forces and their effect on platelet activation and adhesion. Many issues should be considered when studying the flow properties of blood or plasma. Whole blood is well known to behave like a non-Newtonian fluid, with the apparent viscosity decreasing with increasing shear rate. At higher shear rates, whole blood approaches a constant viscosity. The major contributor to the non-Newtonian behavior of whole blood is the formation of rouleaux, or clusters of red blood cells at low shear rates. The plasma itself is less subject to non-Newtonian effects. Therefore, in the current studies, plasma is assumed to behave as a Newtonian fluid with a constant viscosity of 1.2 cP at body temperature (37 °C).

Platelet adhesion and aggregation cause the arrest of bleeding at vascular injury, but they can also cause arterial occlusion at sites of atherosclerosis, complicating cardiovascular diseases [49][53]. Shear rates in flowing blood typically range from 500-1600 s^{-1} for arterioles, from 300-800 s^{-1} for large arteries, and from 800-10,100 s^{-1} for atherosclerotic stenosed arteries [54]. The shear rate at the vessel wall plays an important role and is of great interest in biological processes, including normal physiologic signaling and the pathophysiology of atherosclerosis and thrombosis [55]. The height of

thrombi increases linearly with the increase in wall shear rates and has a denser shell for higher wall shear rates. Platelet buildup is caused by shear rates and the separation by the dynamic force of flow [56]. Study of shear rates provide a different insights of thrombus formation and suggests valuable elucidations for certain clinical physio pathological phenomena, including hemostasis and pathological thrombosis.

2.6 Devices for the Study of Platelet Adhesion

Kantak et al. used a PDMS stamp impression technique (micro molding) to pattern proteins within a channel [57]. They used LbL (layer-by-layer) process to coat the stamp with the protein of interest and were then pressed on to the patterned surfaces in channels. PDMS channels allow protein absorption and are optically clear, which allows platelet adhesion imaging optically through the material. PRP extracted from bovine blood was injected into the channels. Platelets were then labeled with acridine orange (AO). The layered proteins were examined through fluorescent tagging. The flow rate of PRP was controlled by varying fluid shear rate. They indicated that the effects of agonists already present in sample were not accounted for, and they specified the need to form thrombogenic regions to study the role of agents in the inhibition and activation of platelets [57][58][59].

Eshaq used a system that consists of a silicone gasket sandwiched between two Plexiglas blocks with different concentrations of agonists that are produced by platelets after their activation [8]. Channels were cut into the elastomer and the inlet and outlet holes were drilled in the upper Plexiglass plate with fibrinogen coated on to a surface through LbL with PDDA and PSS as polyion. She found that platelet behavior varies

with local concentrations of activating and inhibiting agonists such as ADP and L-Arginine [8][13][14][60].

Watson and Lopez used methods like those used by Eshaq but did not use the same plastic substrate from the elastomer for the LbL processes because as it was not suitable, instead they used glass slides. The AO staining process used lead to nonspecific staining of the surface where surface became stained without subjecting it to platelets indicating false staining. To solve this problem, Lopez introduced a dynamic LbL process which is similar to the standard static LbL process, except the fluid in contact with the surface during layering is in motion. He observed that this surface provides more accurate fluorescence-based estimates of platelet surface coverage [61][62].

Sanakam and Adams repeated the protocols used by Lopez and Watson, but with fibrinogen patterned into patches on the glass slide. They used FITC tagging, to screen the fibrinogen patches unlike the previous studies where PRP was passed through the channels and stained with AO. Their primary research goal was to develop a thrombogenic region surrounded by non-thrombogenic region which would not degrade the fibrinogen surface and would prevent non-specific adhesion of platelets outside of the fibrinogen patches. Therefore, they designed a channel with distinct thrombogenic and non-thrombogenic regions. Xurography was used to make patterns of the thrombogenic and non-thrombogenic regions to produce micro channel. Their work studied fibrinogen only. The study of other proteins that affect platelet adhesion was not practical, because the experiments were time consuming and most of the process had to be done on the same day itself [33][34].

Therefore, the fluid model we proposed used the protocols and micro channel designed by Sanakam and Adams to pattern the protein surfaces of fibrinogen. The platelet adhesion and platelet activation depend on multiple activators and inhibitors that are derived from platelets themselves. Hence the proposed model was used to study combined effects of positive and negative feedback in platelet adhesion by adding platelet-derived activators and inhibitors to platelets adhered on different surface protein fibrinogen.

The experiments reported here are extension of the work done by Sanakam and Adams. Sanakam and Adams built a micro channel patterned with thrombogenic regions and non-thrombogenic region (one that has thrombogenic and non-thrombogenic surfaces side-by-side) to study simultaneous examination of positive and negative feedback effects on regions in which thrombus formation is active next to regions in which thrombus is prevented and got few results which suggests an influence of agents secreted by upstream platelets on downstream adhesion, but some of the results were not statistically significant; additional data was necessary to quantitatively model the effects. Combined effects of positive and negative feedback signals acting at various locations are the main controlling factors of the final thrombus size. Sanakam and Adams did not concentrate on the combined effects of chemical agents and neglected the percent surface area coverage and its effects when production of NO is prevented with the addition of ADP to the plasma along a thrombogenic surfaces. This will be used to test various strategies to inhibit thrombus formation under flow conditions and to minimize the impact on hemostasis.

CHAPTER 3

METHODS

3.1 Experimental Process for Microchannels

To evaluate the adhesion of platelets, a system was used in which micro channels were created with Xurography and patterned on the bottom surface with an isolated thrombogenic fibrinogen region surrounded by a non-thrombogenic region. Platelets were extracted from bovine whole blood and were labeled with CFSE. The CFSE-labeled PRP was perfused through the micro channel under varying conditions. Micro channels were then imaged under a fluorescence microscope and the images were processed with a MATLAB program to determine percent surface area coverage. This procedure was repeated in under various experiments with a varying combinations of activator and inhibitor concentrations under the influence of shear rate.

The flow system is shown in **Figure 3-1**. A syringe pump was used to drive the CFSE-labeled PRP flow into the micro channels. The flow rate and shear rate were controlled using the control panel of the syringe pump.

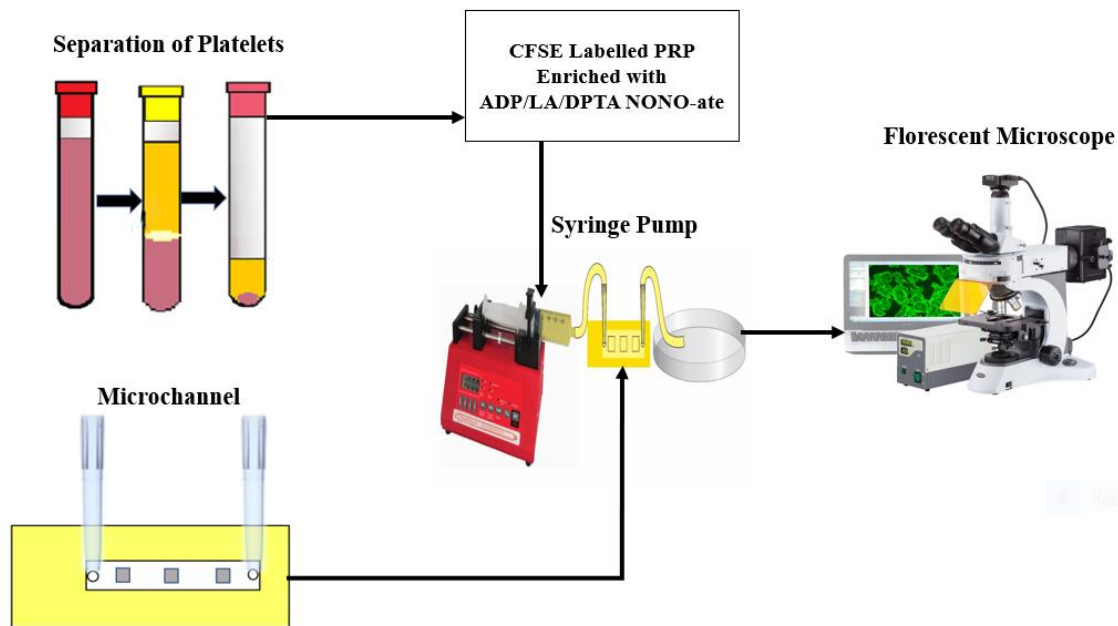


Figure 3-1: Experimental set up for the microchannel flow system.

3.2 Chemicals Used for Both the Protocols

3.2.1 Chemical Preparation

To prepare PBS solution, one packet of PBS (Sigma Aldrich-P3688) was dissolved into 1000 mL of DI water to make a bulk solution. Then bulk solution was stored in the refrigerator until used. Bulk PBS, when used, was poured from into individual 50 mL styrene tubes as to not contaminate the bulk solution.

To prepare CFSE solution, 500 μg CFSE per vial (Sigma Aldrich-21888), 60 μl of dimethyl sulfoxide (DMSO, Sigma Aldrich-276855) was added using a pipet to give a stock solution of 14.9 μM . This solution was prepared immediately before use and used completely each time. Alternatively, 25 mg CFSE was added to 3 mL DMSO to give a final stock solution of 14.9 μM . The solution was aliquoted at 60 μl and stored in the freezer to be thawed just before use.

To prepare a 20 mM CaCl₂ solution, 444 mg CaCl₂ (Sigma Aldrich-C1016) was added to 200 mL of DI water. The solution was stored at 4 °C.

A BSA packet (Sigma Aldrich-P3688) at pH 7.4 was divided up evenly into 14 tubes and stored in the freezer until used. Just before use, each tube was dissolved into 35 mL of DI water to produce a 2% solution.

One tablet of tris buffer saline (Sigma Aldrich-T5030) was added to 37.5 mL DI water and vortexed until the tablet is dissolved. This procedure was repeated 12 times to produce 450 mL tris buffer saline solution. The solution was stored in the refrigerator until used.

Fibrinogen was added to the tris buffer solution in a 2:1 ratio. Stock solution was made by adding 80 mg of fibrinogen (Sigma Aldrich-F8630) to 40 mL of tris buffer solution. The solution was stored in the refrigerator until used.

Four mL of DI water was added to 25 mg of L NMMA in the original bottle and mixed to remove all the L NMMA. The bottle was added to 95 mL of DI water to form a 1 mM solution. The solution was stored at room temperature.

Twenty mL of DI water and 34.8 mg of L-A powder (Sigma Aldrich-A5006) were combined to form a 10 mM stock solution. This solution was diluted by adding 5 mL of the stock solution to 45 mL of DI water in a 50 mL tube. The dilute solution was filtered with a 0.45 µm syringe filter. Solutions were stored at room temperature

DPTA NONOate (Cayman Chemical-825110) was prepared by adding 5.74 mg in 30 ml of 0.01 M NaOH (Fluka Chemika-53339) solution to make it 1 mM stock solution. Alkaline solutions of NONOate in 0.01 M NaOH are stable and stored at 0 °C for 24 hours. The half-life of DPTA NONOate is 5 hours at 220 °C and pH 7.4.

Five ml of PBS and to 2.1 mg of ADP (Sigma Aldrich-A2754) were added and mixed to form a 1 mM stock solution. The solution is stable when stored at 70 °C. ADP was incubated for 15 minutes after adding it to PRP and then perfused through the microchannels.

3.2.2 Bovine Blood Source

Bovine blood was collected from Louisiana Tech University Farm located in Ruston. Blood was withdrawn from a puncture wound made by a 16-gauge needle. The blood was collected in a polystyrene tube that was prefilled with sodium citrate, a calcium chelator, in the ratio of 9:1 by volume i.e., nine parts of blood to one part citrate. Sodium citrate was prepared by adding 16.17 grams of trisodium citrate dihydrate from Sigma Aldrich in 500 ml of deionized water to make it to final concentration of 0.1 M. In addition to binding calcium, citrate helps to maintain the pH value of the blood.

3.2.3 Preparation of PRP

To each 15 ml tube, 4 ml of blood was added and centrifuged at 1500 rpm for 10 minutes. The serum and buffy coat (PRP) from the top of RBC layer was removed and placed in a clean Eppendorf tube. To remove the remaining RBC's, the tube was centrifuged again at 1500 rpm for 3 minutes at 25°C. After removing the left-over RBC's, the PRP was transferred into a clean tube and centrifuged again at 2700 rpm for 10 minutes, forming a platelet pellet. The separated platelet poor plasma (PPP) and platelet pellet were saved in a fresh clean tubes.

3.2.4 CFSE-Labelled PRP

Carboxyfluorescein succinimidyl ester (CFSE) is an ester compound that passes through the membrane of viable cells and cleaved by intracellular esterase to form

fluorescent compound that can be passively injected into the platelets due to its negative charge [63]. Fluorescein derived from CFSE has an amine-reactive succinimidyl group that can covalently bind to proteins or other amino groups in the cell or on its membrane. This covalently attached fluorescein can be analyzed over several weeks [64]. PBS was added to isolated platelet pellet to bring the final volume to 6 ml. 60 mL of CFSE were added and incubated in the dark at room temperature for 10 minutes. It was then centrifuged at 2,600 RPM for 10 minutes. The supernatant was disposed of, and the platelet pellet resuspended into 2 mL of PBS. The isolated PPP was added to the CFSE-labeled platelets and PBS was added to give a final volume of 4 milli Liters.

3.2.5 Preparation of Microchannels

The microchannel system (**Figure 3-2**) includes a silane bottom slide and quartz glass slide top slide. Kapton tape (Kaptonetape-PPTDE-2, Double sided polyimide tape-2' X 36 yds) is cut with a rectangular slit that forms the channel and is sandwiched between the two slides. Two holes were drilled in the quartz slide, and pipette tips were glued to them to provide fluid inlet and outlet ports.

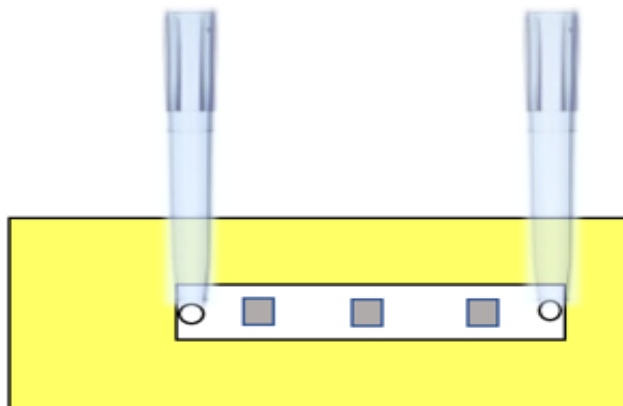


Figure 3-2: The microchannel with inlet and outlet flow units.

3.2.6 Silane Slide Preparation

The silane slides were cleaned with Alconox and dried with nitrogen gas. A Graphtec Craft Robo was used to separate the tape into three regions, A, B, and C, as shown in **Figure 3-3**. Region A is outside of the flow area. Regions B and C are inside the flow area. Region B is to be coated with a non-thrombogenic protein, and Region C is to be coated with a thrombogenic protein. The Kapton tape was removed from region B and incubated with bovine serum albumen (BSA) for two hours to block platelet adhesion on that region; because the silane glass slide surface is hydrophilic, it adsorbs the BSA. Upon removal from the BSA, slides were rinsed gently with DI water and dried with nitrogen gas. The outlines of the regions three 2 mm by 2 mm islands, labeled C were marked with a permanent marker on the back of the slide, and the tape was then removed from these regions.

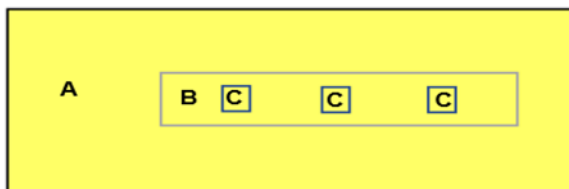


Figure 3-3: Slide with the pre-cut Kapton tape pattern.

Fibrinogen was added with a pipet to these regions, without crossing the outline marked in permanent marker and incubated for one hour. In the final slide the region labeled B was non-thrombogenic (covered with albumen), the regions labeled A were thrombogenic, and the rest of the slide remained covered with Kapton tape as shown in **Figure 3-4**.

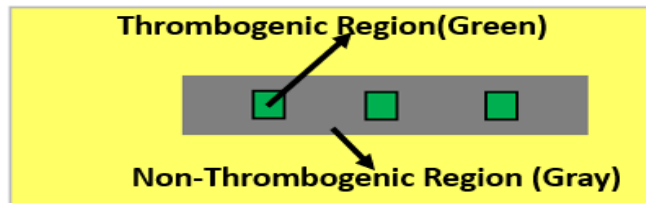


Figure 3-4: Silane Slide patterned with thrombogenic region (green) and non-thrombogenic region (gray).

3.2.7 Quartz Glass Slide Preparation

The plain quartz glass slide was used as the top of the channel. Inlet and outlet holes were cut into the top slide using a DREMEL rotary tool.

3.2.8 Microchannel Fabrication

Each coated Silane slide was used for the base of the channel. The Kapton two-sided tape channel pattern was placed firmly onto the top slide. The plastic covering was removed from the tape and the base slide was pressed firmly on to the tape. The microchannel was placed into a vice and pressed for 10 minutes to bond the channel top and base slides together. Inlet and outlet tubing with inside diameter of 0.091” was attached to the top slide using UV glue.

3.3 **Perfusion of PRP through the Channels**

The syringe pump (Manufacturer – BD, Ref # 309604) drove the PRP through the micro channels at a specific constant flow rate. The flow rates Q were calculated from the equation for Couette flow $Q = wh^2\gamma_w/3$ where w is the width of the channel and h is the height of the channel, γ is the shear rate at the wall [65]. After the PRP is perfused through microchannel, PBS is used to rinse the remaining PRP out of the channel at $1/10^{\text{th}}$ of the plasma perfusion shear rate.

3.4 Mathematical Modeling of PRP Flow in Micro Channels

The most common forces related to platelet adhesion studies are shear stress, τ , measured in dynes/cm² and shear rate, γ , s⁻¹. Shear stress is defined as the force per unit area exerted in the direction of the flow.

Shear stress can be expressed as

$$\tau = -\mu \frac{dv_z}{dr} \quad \text{Equation 3-1}$$

where μ is the viscosity and dv/dr is the local velocity gradient or shear rate. Or, since $\gamma = dv_z/dr$,

$$\tau_w = \mu\gamma, \quad \text{Equation 3-2}$$

and shear stress near the wall of tubular vessels (e.g., the tubes leading to the microchannel) is expressed as function of the volumetric flow rate Q , for which

$$\tau = \frac{4\mu Q}{\pi r^3}$$

The flow of PRP in micro channels is modeled as the PRP flow between two fixed parallel plates as illustrated in **Figure 3-6**.

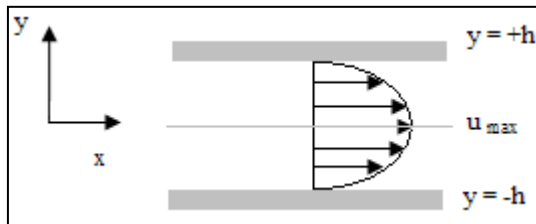


Figure 3-5: Flow between two fixed parallel plates.

From the above model, we can assume Couette flow, where the following equation apply

$$Q = \frac{2u_{\max}hw}{3} \quad \text{Equation 3-3}$$

and

$$\tau_w = \frac{2\mu u_{\max}}{h} \quad \text{Equation 3-4}$$

hence from Equations 3-2 through 3-4,

$$Q = \frac{wh^2\gamma_w}{3},$$

where, w is the width of the micro channel and h is the half the height of micro channel.

3.5 Addition of Activators and Inhibitors

Adding activators and inhibitors modulates the extent of platelet adhesion. The activator ADP (Sigma-Aldrich) was added to PRP before the experiment and incubated for 10 mins. The inhibitors, L-Arginine and DPTA NONOate were also added to PRP to test the effect of inhibitors on platelets. Ca^{2+} is used as an indicator for platelets activation and will be added for the activation of platelets. Therefore, CaCl_2 is added for recalcification of PRP before perfusing PRP into micro channel along with activators and inhibitors.

3.5.1 Effects of ADP and NO on Platelets

The aim of the first set of experiments was to test the effect of various concentrations of ADP and NO on platelet adhesion and aggregation. The project was divided in to three parts.

First, the effect of NO on platelet adhesion to fibrinogen-coated microchannel with thrombogenic and non-thrombogenic regions on it was studied. This study used two methods of nitric oxide production, one endogenous and one exogenous. Endogenous production that was enabled by the addition of L-Arginine, a precursor for NO production through NOS. Exogenous production was enabled by the addition of the NO donor DPTA NONOate to the CFSE-labelled PRP.

The second part of the project examined the effect of ADP alone on platelets adhesion. ADP was added to PRP at different concentrations and incubated for 15 minutes.

For the third part of the project, the combined effect of ADP and NO was examined. Both ADP and L-Arginine or DPTA NONOate were added to the PRP before it was perfused in the microchannels. For each of three concentrations of ADP, 2 μM , 5 μM , and 10 μM , three concentrations of LA were used, 5 μM , 10 μM , and 15 μM . The same concentrations of ATP were combined with 5 μM , 10 μM , and 15 μM of DPTA-NONOate.

3.6 Syringe Filling

Each syringe was filled based on the experiment in the order below and then secured into the syringe pump.

Table 3-1: Summary of Parameters used in experiments.

PRP (mL)	CaCl ₂ (μL)	ADP (μL) Incubation for 15 minutes	L-A (μL)	DPTA NONOate (μL)
3	400	0 6 15 30		
3	400		0 15 30 45	
3	400			0 15 30 45
3	400	0 6 15 30	0 15 30 45	
3	400	0 6 15 30		0 15 30 45

CaCl₂ was added to recalcify the PRP because Ca²⁺ is a known indicator of platelet activation and therefore necessary for the activation of platelets. After perfusion of CFSE labeled PRP, the inlets and outlets of the microchannels were removed, including glue, and washed with Alconox soap and left it to dry for 5 minutes.

3.7 Calculation of NO Concentration from an NO Donor

We have used DPTA NONOate, an exogenous NO donors in this work with half-life of about 5 hours. While the exact concentration of NO can be measured via the electrochemical probes and can be deduced from the Nitrate/Nitrite assay, it is useful to have a mathematical model for the NO concentration in the solution as a function of time. Assuming that the donor and NO both decay exponentially in time and that the half-life for NO is much shorter than that for the donor, a balance of production and decay of NO yields the simple equation:

$$[NO] = \frac{\tau_{NO}}{\tau_D} [D_0] e^{-t/\tau_D} \quad \text{Equation 3-5}$$

where $[NO]$ is NO concentration, $[D_0]$ is the initial donor concentration, and τ_{NO} and τ_D are the exponential decay times (proportional to the half-life) for NO and the donor, respectively. For a given a NO donor, DPTA NONOate with a half-life of 5 hours, the initial NO concentration will be approximately 0.54×10^{-3} times the initial donor concentration (millimolar concentrations of donor yield nanomolar concentrations of NO). The expected concentration of NO, for the given the concentrations of 5, 10, and $15\mu\text{M}$ DPTA NONOate were 2.7, 5.4, and 8.1nM respectively which were greater than the minimum NO concentration required to inhibit platelets under all conditions that is 0.15nM [66].

3.8 Fluorescent Microscopy

Olympus 1X51 fluorescent microscope was used to image the thrombogenic and non-thrombogenic regions of interest at a magnification of 20X, and FITC and TRITC filters. The regions imaged are shown in **Figure 3-6**. Regions T1, T2 and, T3, in the direction of flow, were the 2 mm by 2 mm dots on the silane slide. Regions NT1 and

NT2, from upstream to downstream, were the two non-thrombogenic regions. The images from each experiment were saved and processed through the MATLAB image processing program to calculate the percent surface area coverage.

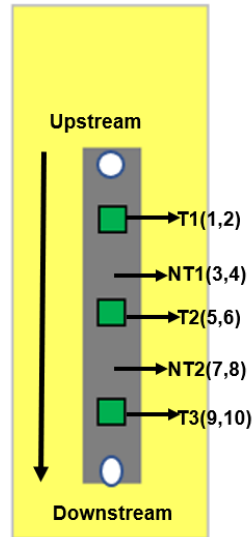


Figure 3-6: Nomenclature for the images taken from the slide.

3.9 Experimental Process for Calcium Imaging

Calcium concentration is very low (~ 100 nM) in the cytosol of a cell and is highly concentrated (~ 2 mM) at intracellular calcium stores such as endoplasmic reticulum (ER) and extracellular spaces creating a difference in calcium concentration which is effectively utilized to deliver signals across the cell membrane. This implies that activating calcium signaling with any stimulus leads to release of calcium from these stores following increase in calcium concentration of cytosol. The calcium released in the cytosol is either actively taken up by the ER via calcium channels called Sarco-Endoplasmic reticulum Ca^{2+} -ATPase (SERCA) or it is flushed out through calcium channels present in plasma membrane. During these processes, calcium transients/spikes are formed, which are characterized by the rise and fall of calcium concentrations in the

cytosol repeatedly. Experiments were performed to monitor changes in cytosolic calcium level in platelets that were loaded with a calcium-sensitive fluorophore Fluo-4 AM. Fluo-4 AM is a cell permeant variant of Ca^{2+} indicator which increases the fluorescence intensity upon binding to calcium.

3.9.1 Chemicals Used in Calcium Signaling in Platelets

Calcium indicator dye, Fluo-4 AM, was obtained from Invitrogen and used in calcium imaging experiments. Locke's solution used here was prepared in the Dr. Decoster's lab following Locke's protocol. All agonists and other chemical agents used in experiments were bought in powder form (Sigma) except exogenous NO donor DPTA NONOate, which was brought from Cayman Chemical. Preparation methods were given in Section 3.2. Ionomycin (Iono) is the calcium ionophore that facilitates the movement of calcium in and out of the cells, is used as a positive control for calcium influx in the cells.

3.9.2 Platelet Extraction

Platelets were separated from bovine blood brought from Louisiana Tech Farm using centrifuge method. The extracted platelet pellet was suspended in 4 ml of PBS.

3.9.3 Treating Platelets with Calcium Ion Indicators

The collected platelets in PBS were treated with Fluo-4 calcium ion indicator and then the solution was allowed to settle down inside the incubator at 5% of CO_2 and 37 °C for about 15-20 mins. Loading solution (Lock solution) of 3 ml with 3 μl of pluronic acid with 5 μl of Fluo4 calcium indicator was added and incubated for 1 hr. Later, 500 μl of recovery solution was added to each of three wells and incubated for 45 mins. Then we removed the recovery solution from each well expecting at least platelets settled at the bottom of the well.

3.9.4 Calcium Activity in Platelets with Platelet Activators and Inhibitors.

The objective of these experiments was to see how platelet activators and inhibitors affect the calcium activity in platelets. Platelets were treated with an activator ADP, exogenous NO donor, DPTA NONOate, and L-Arginine, which acts as endogenous NO donor, in the presence external calcium.

3.9.5 Calcium Imaging After Treatment with Chemical Agents

The cells were imaged after the recovery period while being stimulated with ADP, and ionomycin to induce calcium signaling. Chemicals L-Arginine and DPTA NONOate were added after stimulating platelets with ADP. Fluorescent intensity changes in the cells in real-time, which corresponds to the calcium influx due to stimulation via agonist, was imaged and recorded in real-time under the inverted microscope (Olympus CKX41) with a 488 nm excitation wavelength filter at a frame rate of 4 seconds. The experiment was visualized and recorded in the Intracellular Imaging software (InCyt Im™ Imaging system, Version 5.29e, Cincinnati, OH).

After treating platelets with ADP/L-A/DPTA NONOate, there was a small dilution artefact observed, where the calcium peak goes down and comes back to its base position with increase in fluorescent intensity with respect to the agonists added. These artefacts which shows small decrease in fluorescent intensity and accounts to fall in calcium peaks were corrected by analyzing the results for all the cells that showed calcium response above the normalized threshold fluorescence values i.e., 1.2 or 20% above baseline for all agonist stimulations.

3.9.6 Measuring and Analyzing Calcium Fluorescence Intensity

The recorded experiments were analyzed in InCyt Im™ Imaging System software set up in Dr. DeCoster's lab. Regions of interests (ROIs) termed as 'Trial' in the graphs obtained from the experiments and were created as a circle around each cell identified in a frame. ROIs with maximum fluorescence caused by ADP stimulation were selected to maximize the visualization and analysis of the number of cells in the frame. The fluorescence intensity of each cell over time were measured for the ROIs selected and the data obtained were then normalized to their starting values (baseline) in Microsoft Excels. The normalized values of fluorescence intensity over time are represented by line graphs and are used to compare cells within the experiment or to other experiments. The averages of peak fluorescence intensity were calculated for each experiment, and the values were averaged over 3 experiments.

3.10 Statistical Analysis

The single factor Analysis of Variance (One-way ANOVA) was performed to analyze the effect of different concentrations of ADP/L-A/DPTA NONOate on overall PSAC of the microchannel and two factor Analysis of Variance (Two-way ANOVA) was performed to analyze the effect of PSAC for different concentration of ADP/L-A/DPTA on three different thrombogenic regions T1, T2, and T3 respectively. A 95% confidence interval and corresponding $\alpha = 0.05$ threshold was used. If the P values for the test is less than the $\alpha = 0.05$ it means that F-statistic value is very large, higher than the critical value indicating that the null hypothesis for single factor ANOVA, the means of overall PSAC for three concentration of agonist (5, 10, and 15 μM) are same, is rejected.

The two factor ANOVA was performed to analyze the effect of PSAC on microchannels by two factors, one of them was the thrombogenic regions from upstream to downstream (T1, T2, and T3) and the other factor was the ADP/L-A/DPTA NONOate concentrations (2, 5, and 10 μ M). The three-null hypothesis for two-way ANOVA were the means of PSAC grouped by one factor (different thrombogenic regions T1, T2, and T3) are same and the means of PSAC grouped by another factor (different concentrations of chemical agents) are same and that there exists no interaction between two factors for the $\alpha = 0.05$ level. This help us to analyze if there is a any significant difference in the adhesion characteristics among different thrombogenic regions with release of antagonists with different concentrations. If the p values for three null hypothesis for the test are less than the $\alpha = 0.05$ indicates that there is statistical difference in means of PSAC for thrombogenic regions T1, T2, and T3 and for different concentrations of chemical agent and says there exists interaction between two factors and depends on each other for the $\alpha = 0.05$ level. A logarithmic transformation was used to determine the statistical difference between the small values on the non-thrombogenic regions against the larger values on the thrombogenic regions, because the large standard deviation in the case of the thrombogenic region is too large to rule out zero as a mean, even though all values are above zero and substantially larger than all the values on the non-thrombogenic region [67].

CHAPTER 4

RESULTS

4.1 Platelet Surface Area Coverage

Images from thrombogenic and non- thrombogenic regions of the microchannel after perfusion of CFSE-labeled platelets with no chemicals at a shear rate 1500 s^{-1} were collected and processed through the MATLAB program to calculate the percent surface area coverage. **Figure 4-1** shows sample images of thrombogenic and non-thrombogenic regions of the microchannel (Region A and B) as identified in **Figure 3-6**.

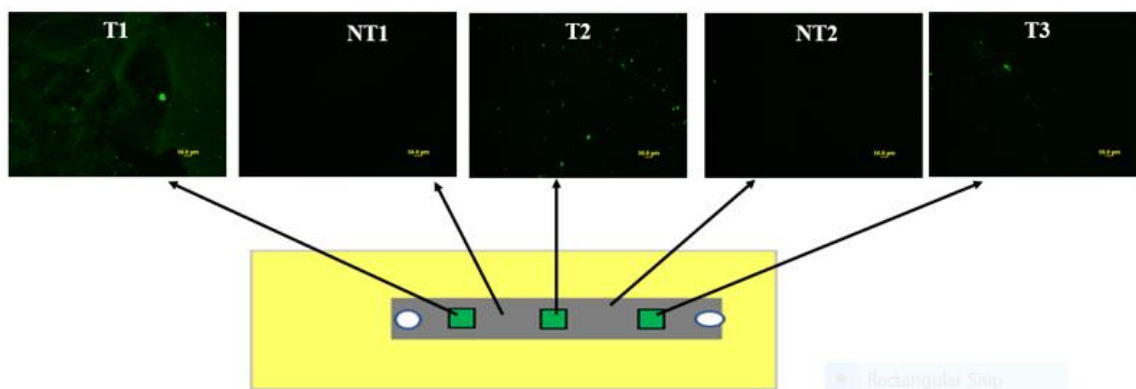


Figure 4-1: Overall adhesion of platelets from upstream to downstream regions of the microchannel.

Green portions on these images that were above a threshold intensity value of 30 were extracted and represented as white areas, while the other regions were represented with black in binary images, as shown in **Figure 4-2**. Image A in **Figure 4-2** shows platelets adhered to fibrinogen patterned on thrombogenic region of the base slide after

perfusion CFSE-labeled platelets and Image B was its binary image. The overall percent surface coverage of Image B (white area divided by total area times 100) is 0.89.

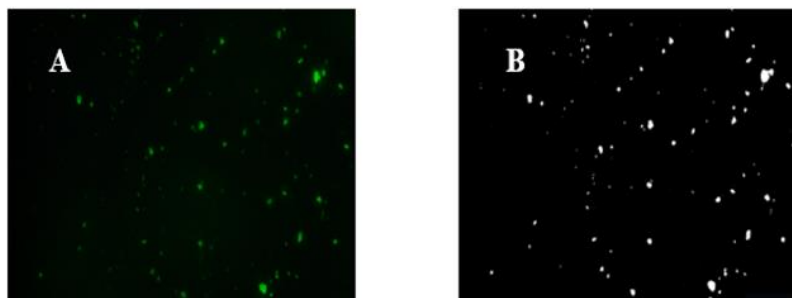


Figure 4-2: Image A is first image of region T1 from the base slide perfused with CFSE labeled platelets with no chemical at a shear rate of 1500 s^{-1} . A) Original image, B) Binary Image.

Figure 4-3 is another image, where most of the entire surface (62.2%) is covered with green florescence. The binary image with the white color as shown in Image B.

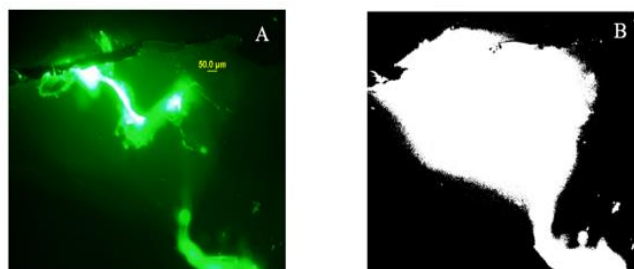


Figure 4-3: Sample Image from the base slides, with no chemical added, perfused with CFSE labeled platelets at a shear rate of 1500 s^{-1} . Overall average percent surface coverage is 62.2. A) Unprocessed image B) Binary of Image A.

Figure 4-4 is another image, where the florescence image surface is covered except for a region at the left side of the image. The surface coverage is 93.35%.

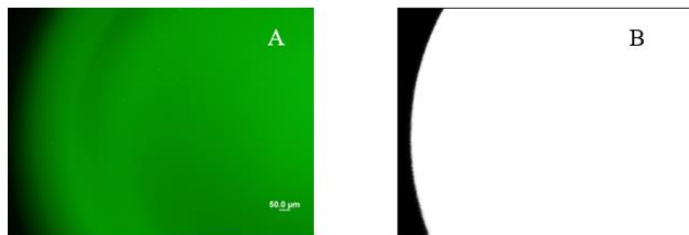


Figure 4-4: Image from the base slides, with no chemical added, perfused with CSFE labeled platelets at a shear rate of 1500 s^{-1} . Overall average percent surface coverage is 93.0 A) Original image, B) Binary of Image A.

The non-thrombogenic region was imaged in FITC to show the BSA surface and fibrinogen regions. **Figure 4-5** shows contrast between the two regions where fibrinogen regions surrounded by BSA adhered to silane slide surface. Image A represents the region covering T1, on the left, and NT1, on the right, and Image B is the region covering T2, on the left, and NT2, on the right, of the sample base slide.

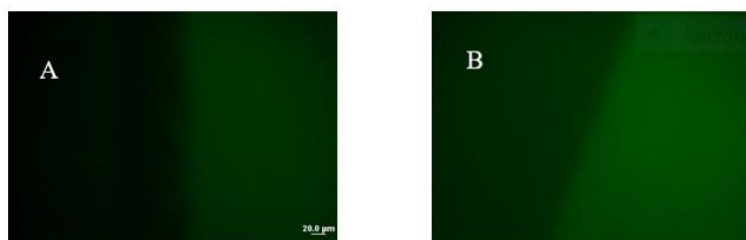


Figure 4-5: Slide imaged in FITC after addition of the fibrinogen. The tagged fibrinogen (green) is to the left, and the blocked BSA (black) region is to the right for both image A (Region covering NT1 and T2) and image B (region covering NT2 and T3).

Different concentrations of exogenous and endogenous chemical agents with shear rate of 100 s^{-1} on 5 mm channel width and 2 mm by 2 mm of thrombogenic region size were investigated in these experiments. Different samples of blood (collected from the same animal on different days) were used to study the combined effects of positive and negative feedback on micro channel. Based on the initial experiments the concentrations 0, 5, 10, and 15 μM of LA and DPTA NONOate with 0, 2, 5, and 10 μM

were used in the experiments. For each experimental trial, different samples of blood were used to determine the effects of chemical agents. Three sets of experiments for each effect were completed to test each hypothesis.

4.2 Experiment Controls

Our key criteria in designing microchannel was that fibrinogen and platelets should not bind to the non-thrombogenic regions. BSA was selected as blocking agent in creating non-thrombogenic regions because it effectively blocks the binding of both fibrinogen and platelets to the silane slide. It was also necessary to verify the BSA, untagged fibrinogen, untagged platelets do not show fluorescence and need to ensure that FITC signal was specific to CFSE-labeled platelets. **Figure 4-6** shows images were taken of the silane slide under an FITC filter at each step of process during experiments, before addition of BSA, after addition of BSA, after addition of fibrinogen, and after perfusion of labeled and unlabeled PRP. The images showed no fluorescence within the fibrinogen regions.

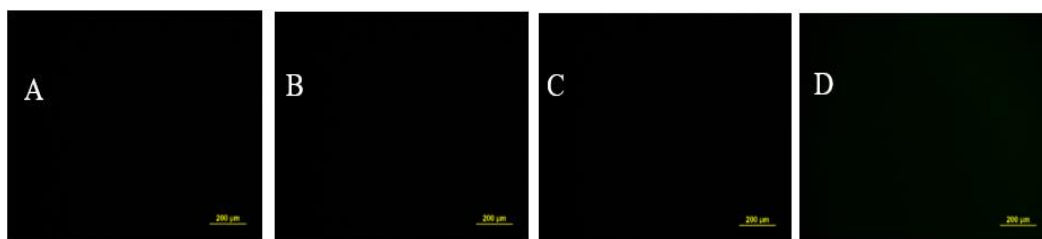


Figure 4-6: Images of the fibrinogen regions at each step of the experimental process. Image A: blank slide. Image B: after addition of BSA. Image C: after addition of untagged fibrinogen. Image D: after perfusion with unlabeled PRP.

Images of non-thrombogenic region, the region surrounding the thrombogenic regions showed little to no fluorescence after perfusion with CFSE-labeled platelets, verifying their non-thrombogenicity (**Figure 4-7**).



Figure 4-7: Control images of non-thrombogenic regions after perfusion of channels with CFSE labelled platelets, as recorded from four different experiments. Image A: No Chemical Added, Image B: ADP added, Image C: L A added, Image D: DPTA NONOate.

Images of non-thrombogenic regions also showed fluorescence only when the coated fibrinogen was outside the thrombogenic region and the non-thrombogenic region. This problem occurred because of inaccuracy in coating fibrinogen on 2 mm by 2 mm thrombogenic patches that had been covered by Kapton tape and manually marked with a Sharpie. Sample images are shown in the **Figure 4-8**.

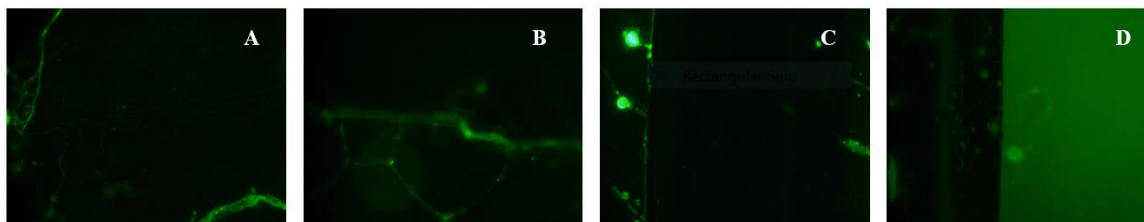


Figure 4-8: Sample images from non-thrombogenic regions (Images A & B are from NT1; Images C and D from NT2) when fibrinogen is outside of the marked region.

4.3 Effect of ADP Concentrations on Platelet Surface Area Coverage

ADP is a well-known activator that enhances contact-induced activation of platelets. ADP in concentrations of 2, 5, and 10 μM was added to CFSE-labeled PRP consecutively according to the protocol described in the methods section. The CFSE-labeled PRP was perfused through microchannels at a constant shear rate of 1500 s^{-1} . Fluorescent images of the microchannels were collected for each ADP concentration and

repeated at least three times at constant shear rate to see the good amount of platelet adhesion to the thrombogenic regions patterned with fibrinogen.

The collected fluorescent images were processed using MATLAB code to see the percentage surface area coverage (PSAC). Sample fluorescent images of the microchannels, after perfusion CFSE-labeled PRP, are shown in **Figure 4-9**. The base slides were perfused with CFSE-labeled platelets with different concentrations of ADP (0, 2, 5, and 10 μM , from top to bottom row) at a shear rate 1500 s^{-1} . The three thrombogenic regions are upstream (T1), middle (T2), and downstream (T3). Non-thrombogenic region NT1 is between regions T1 and T2, and non-thrombogenic region NT2 is between regions T2 and T3. Both platelet adhesion and thrombus size increased with increased ADP concentration. The PSAC averaged over the three thrombogenic regions for each ADP concentration is shown in **Figure 4-10**. The error bars represent the standard deviation over all trials and all three regions. The charts in this dissertation used logarithmic scale. These results were consistent with the acceleration of platelet recruitment by ADP.

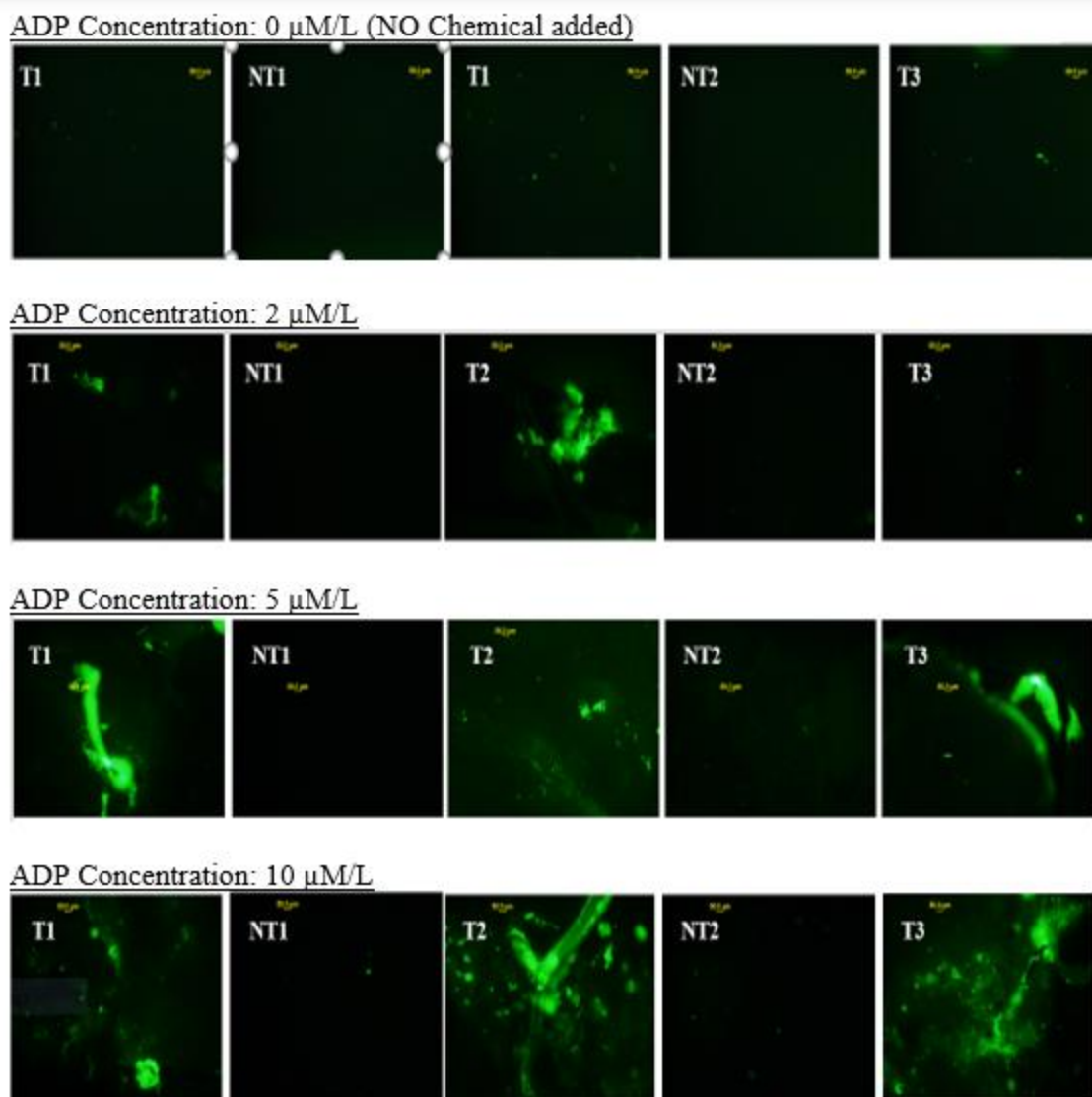


Figure 4-9: Platelet adhesion under different concentrations of ADP 0, 2, 5 and, 10 μ M/L in first, second, third and, fourth row, respectively. Images T1, NT1, T2, NT2, and T3 in each row represents nomenclature for the images taken from the slide as mentioned in Figure 4-1 and Figure 3-6.

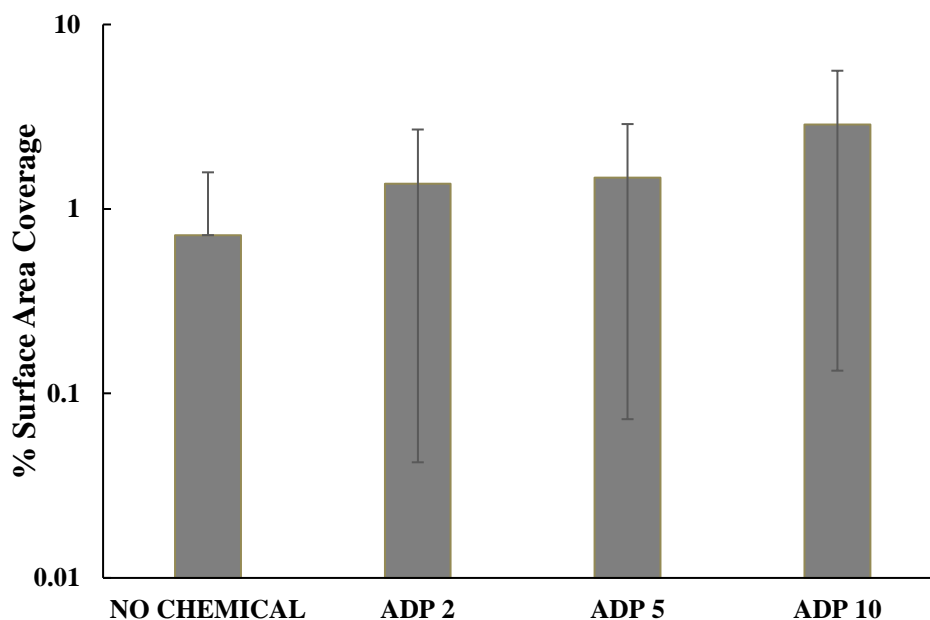


Figure 4-10: Experimental results on overall percent surface area coverage with no chemical, 2 $\mu\text{M/L}$ ADP, 5 $\mu\text{M/L}$ ADP, 10 $\mu\text{M/L}$ ADP added perfused at a shear rate of 1500 s^{-1} . Error bars represent standard deviation.

Figure 4-11 shows platelet adhesion at different concentrations of ADP from upstream to downstream. The PSAC is shown on a logarithmic scale to allow the small values on the non-thrombogenic regions to be plotted along with the larger values on the thrombogenic regions. Except for the case of $10 \mu\text{M}$, adhesion increases from T1 to T2 and then decreases at T3. Fluorescence on NT1 and NT2 was minimal. For the $10 \mu\text{M}$ PSAC increased monotonically from upstream to downstream.

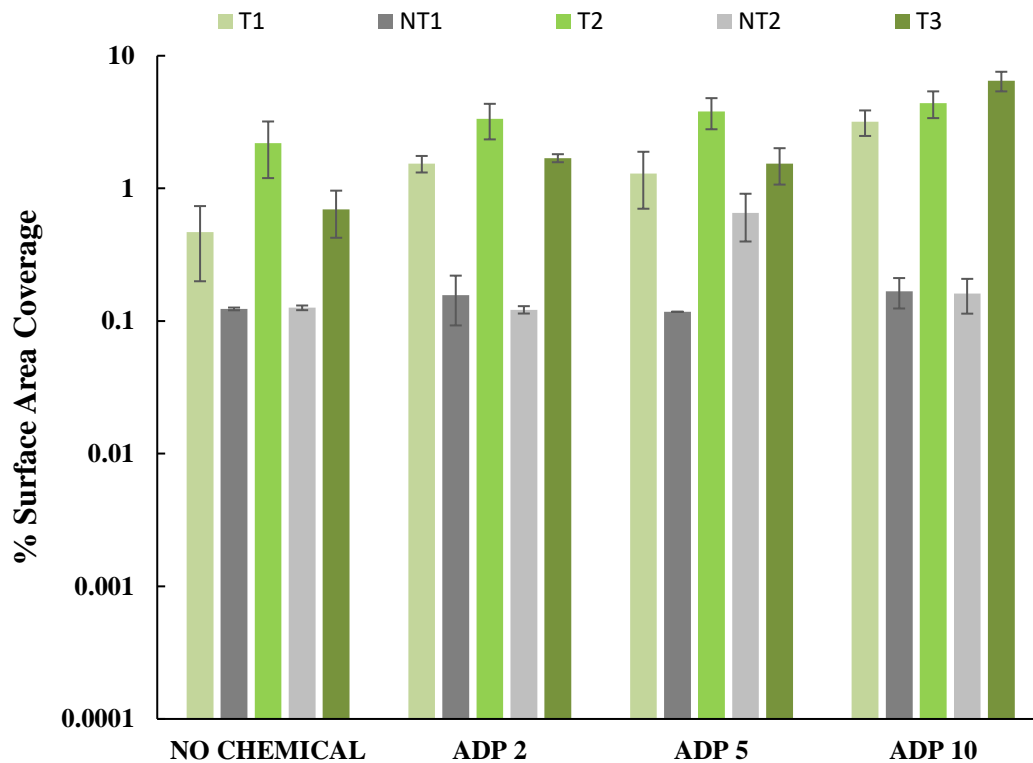


Figure 4-11: Experimental results on effect of percent surface area coverage for different concentration of ADP on microchannel from upstream to downstream say T1-NT1-T2-NT2. Error bars represent standard deviation.

4.3.1 Statistics

The ANOVA single factor and two factor test analysis was performed to analyze the effect of different concentrations of ADP on overall PSAC and to analyze the effect of PSAC for different concentration of ADP on microchannel from upstream to downstream on three different thrombogenic regions T1, T2, and T3 respectively. The single factor analysis of variance shows the statistical significance difference between the means of overall PSAC for three different concentration of ADP 2, 5, and 10 μ M. The P values for the test was 0.000315 which is less than the $\alpha = 0.05$ it means that F-statistic value is very large, higher than the critical value indicating that the null hypothesis for

single factor ANOVA is rejected. This p value suggested a significant difference in the adhesion characteristics among ADP concentrations.

The two factor ANOVA was performed to analyze the effect of PSAC on microchannels by two factors, one of them was the thrombogenic regions from upstream to downstream (T1, T2, and T3) and the other factor was the ADP concentrations (2, 5, and 10 μ M). The p values for three null hypothesis are 0.002, 0.000000426, and 0.03 indicating that there is statistical difference in means of PSAC for thrombogenic regions T1, T2, and T3 and for different concentrations of ADP 2, 5, and 10 μ M and says there exists interaction between two factors and depends on each other for the $\alpha = 0.05$ level. This led us to believe that there is a significant difference in the adhesion characteristics among different thrombogenic regions with release of agonists and their concentrations.

4.4 Effect of L-Arginine on PSAC

L-A was added to the CFSE-labeled PRP in four concentrations (0, 5, 10, and 15 μ M) before perfusion through the microchannel at a shear rate of 1500 s^{-1} . **Figure 4-13** is a montage of sample images of the microchannel base slide from this study. The columns from left to right are regions T1, NT1, T2, NT2, and T3. L-A concentrations are 0 μ M (first row), 5 μ M (second row), 10 μ M (third row), and 15 μ M (fourth row). Adhesion is easily seen in the 5 μ M images and becomes sparse at all locations at 10 and 15 μ M concentrations.

L-A Concentration: 0 μ M



L-A Concentration: 5 μ M



L-A Concentration: 10 μ M



L-A Concentration: 15 μ M



Figure 4-12: Platelet adhesion under different concentrations of L-A 5,10 and, 15 μ M/L in first, second, third and, fourth row, respectively. Images T1, NT1, T2, NT2, and T3 in each row represents nomenclature for the images takem from the slide as mentioned in Figure 4-1 and Figure 3-6.

Figure 4-13 shows the overall percent surface area coverage for this study, averaged over the three thrombogenic regions and over three experiments for each L-A concentration. The mean values gradually decrease with L-A concentration.

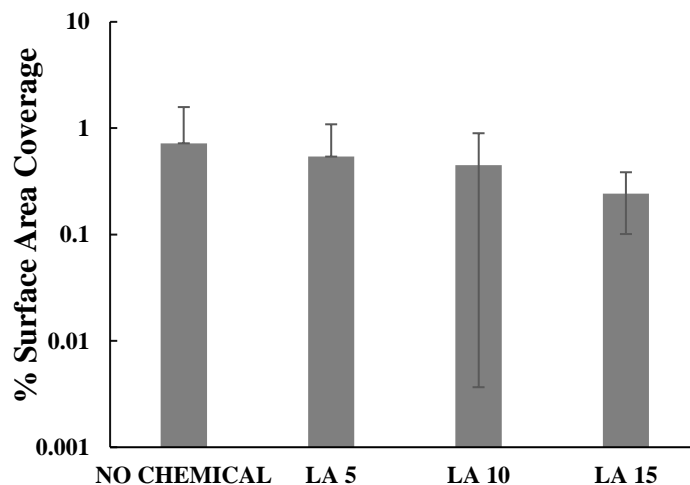


Figure 4-13: Experimental results on overall percent surface area coverage with 0, 5, 10, and 15 μM L-A added at a shear rate of 1500 s^{-1} . Error bars represent standard deviation.

Figure 4-14 shows adhesion divided into the different thrombogenic and non-thrombogenic regions. When L-A is added, the middle thrombogenic region tends to have a smaller PSAC than the other two. T1 has a greater PSAC than T3 at 5 μM , but a smaller PSAC than T3 at 10 and 15 μM . The non-thrombogenic regions show minimal adhesion at all L-A concentrations.

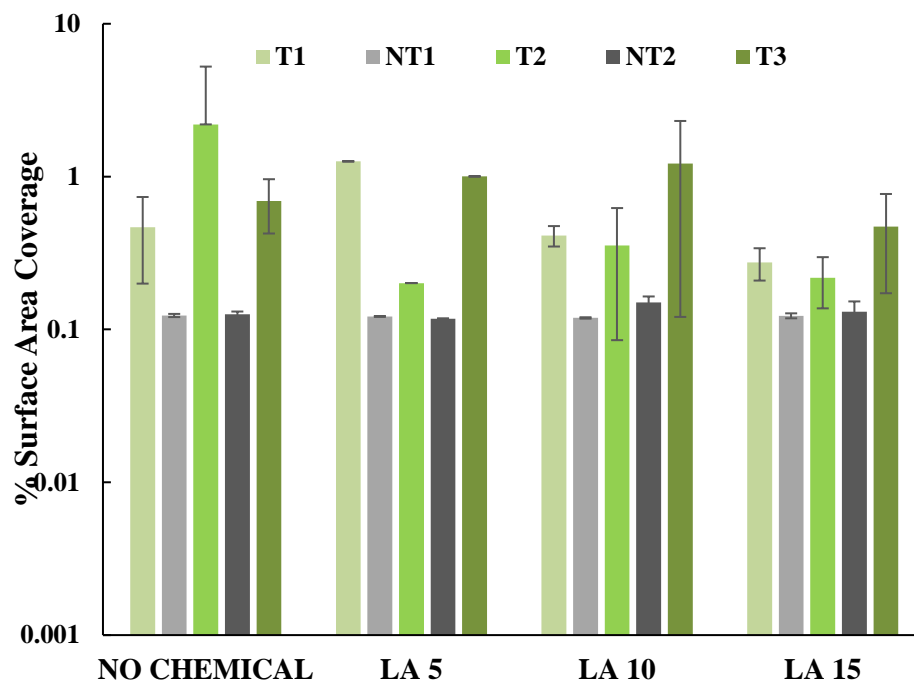


Figure 4-14: Experimental results on effect of percent surface area coverage for different concentration of L-A on microchannel from upstream to downstream say T1-NT1-T2-NT2. Error bars represent standard deviation.

4.4.1 Statistics

The PSAC decreased with increase in the concentration of L-A, with all values being lesser than 1% at high concentration of L-A. The ANOVA single factor and two factor test was performed to analyze the effect of different concentrations of L-A on overall PSAC and on different thrombogenic regions of microchannel respectively.

The single factor analysis of variance shows the statistical significance difference between the means of overall PSAC for three different concentration of L-A 5, 10, and 15 μ M. The P values for the test was 0.0256 which is less than the $\alpha = 0.05$ and F-statistic value is higher than the critical value indicating that the null hypothesis for single factor ANOVA is rejected. This p value suggested a significant difference in the adhesion characteristics among L-A concentrations.

The two factor ANOVA was performed to analyze the effect of PSAC on microchannels by two factors, one of them was the thrombogenic regions from upstream to downstream (T1, T2, and T3) and the other factor was the three different L-A concentrations (5, 10, and 15 μ M). The p values for three null hypothesis are 0.33, 0.003, and 0.17 indicating that there is no statistical difference in means of PSAC for thrombogenic regions T1, T2, and T3 and for different concentrations of L-A and tells there exists no interaction between two factors for the $\alpha = 0.05$ level. This led us to believe that there is a no significant difference in the adhesion characteristics among different thrombogenic regions with release of antagonists with different concentrations.

4.5 Effect of DPTA NONOate on PSAC

The high diffusion coefficient of NO and consequence of its small size has a significant role in inhibiting activated platelets. To test the effect of NO in our system, we added DPTA NONOate, an NO donor, at concentrations of 0 (control), 5, 10, and 15 μ M to the CFSE-labeled PRP. The shear rate was 1500 s^{-1} .

Figure 4-15 is a montage of sample images of the microchannels of both thrombogenic and non-thrombogenic regions along the length of microchannel from upstream to downstream perfused with different concentrations DPTA NONOate added in CFSE-labeled PRP. DPTA NONOate concentration increases from the top row to the bottom row. Platelet adhesion initially decreased as the concentration of DPTA increased.

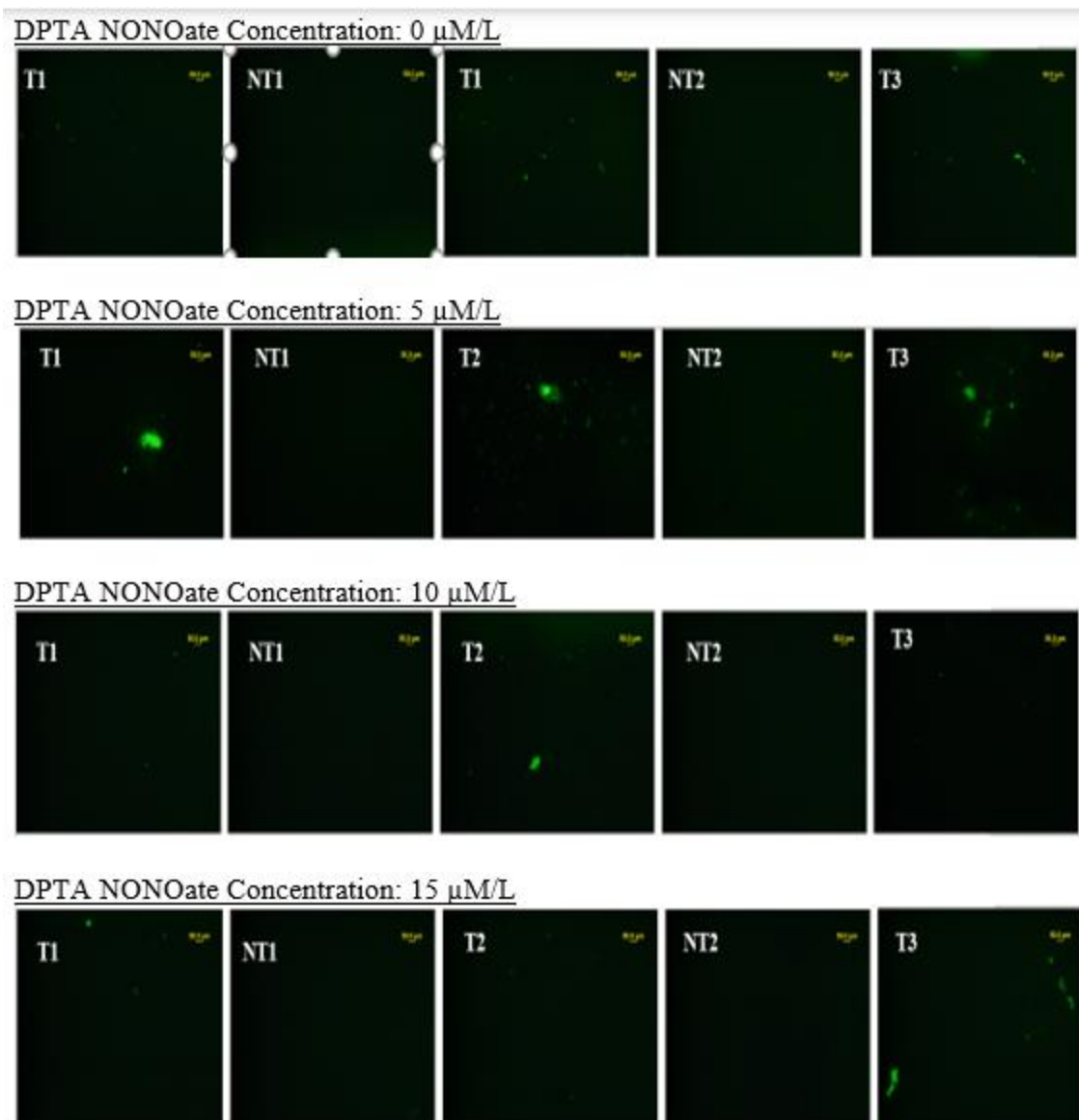


Figure 4-15: Platelet adhesion under different concentrations of DPTA NONOate 0, 5, 10 and, 15 $\mu\text{M/L}$ in first, second, third row, and fourth row respectively. Images T1, NT1, T2, NT2, and T3 in each row represents nomenclature for the images taken from the slide as mentioned in Figure 4-1 and Figure 3-6.

Figure 4-16 shows the overall percent surface area coverage for each concentration of DPTA. Each concentration of DPTA was repeated at least three times with different blood samples, collected from the same animal on different days. Error bars are the standard deviations for the three experiments. The PSAC for high

concentrations of DPTA NONOate did not exceed the percent surface coverage for the control. Thus, platelet adhesion was still inhibited at high DPTA concentrations.

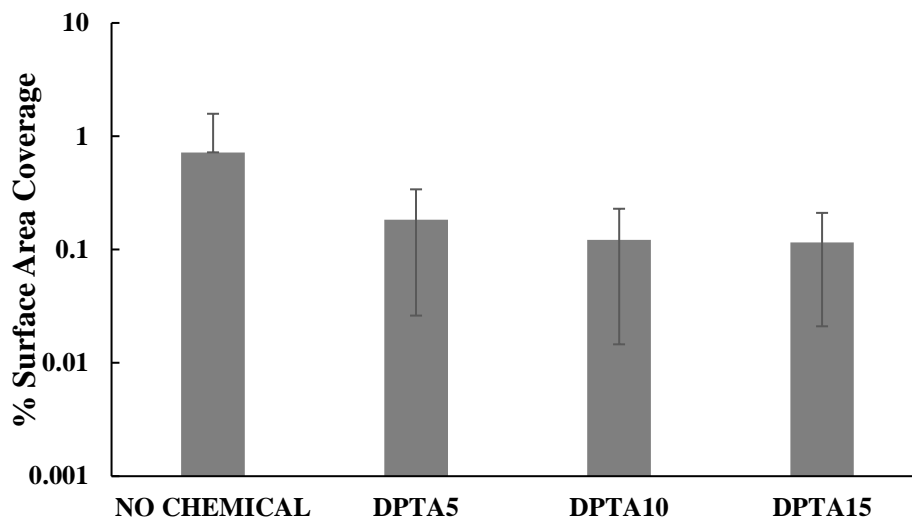


Figure 4-16: Experimental results on overall percent surface area coverage with 0, 5, 10, 15 $\mu\text{M/L}$ DPTA NONOate added to the PRP, which was then perfused at a shear rate of 1500 s^{-1} . Error bars represent standard deviation.

Figure 4-17 shows PSAC for different concentration of DPTA NONOate on the five microchannel regions from upstream to downstream. The PSAC pattern was not consistent with the effect of DPTA NONOate concentrations on the microchannel along the length of upstream to downstream. At lower concentrations i.e., $5\text{ }\mu\text{M}$ of DPTA NONOate, PSAC decreased from T1 to T2 regions and increased from T2- T3. The PSAC along the thrombogenic regions from upstream to downstream is an irregular pattern and not consistent with the increase concentrations of DPTA NONOate.

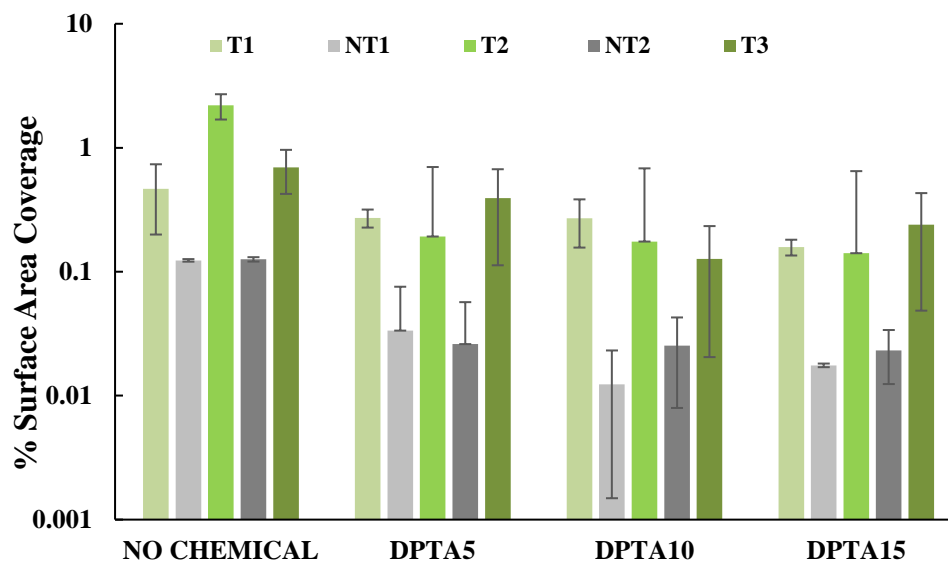


Figure 4-17: Experimental results on effect of percent surface area coverage for different concentration of DPTA NONOate on microchannel from upstream to downstream say T1-NT1-T2-NT2. Error bars represent standard deviation.

4.5.1 Statistics

The PSAC decreased with increase in the concentration of DPTA NONOate. The ANOVA single factor and two factor test was performed to analyze the effect of different concentrations of DPTA NONOate on overall PSAC and on different thrombogenic regions of microchannel respectively.

The single factor analysis of variance shows the statistical significance difference between the means of overall PSAC for three different concentration of DPTA NONOate 5, 10, and 15 μ M. The P values for the test was 0.00037 which is less than the $\alpha = 0.05$ and F-statistic value is higher than the critical value indicating that the null hypothesis for single factor ANOVA is rejected. This p value suggested a significant difference in the adhesion characteristics among DPTA NONOate concentrations.

The two factor ANOVA was performed to analyze the effect of PSAC on microchannels by two factors, one of them was the thrombogenic regions from upstream

to downstream (T1, T2, and T3) and the other factor was the three different DPTA NONOate concentrations (5, 10, and 15 μ M). The p values for three null hypothesis are 0.54, 0.10, and 0.49 indicating that there is no statistical difference in means of PSAC for thrombogenic regions T1, T2, and T3 and for different concentrations of DPTA NONOate and says that there exists no interaction between two factors for the $\alpha = 0.05$ level. This led us to believe that there is a no significant difference in the adhesion characteristics among different thrombogenic regions with release of antagonists with different concentrations.

4.6 Combined Effect of ADP and LA on PSAC

Because ADP is a platelet activator and L-Arginine is a precursor for NO, a platelet inhibitor, it is important to determine the combined effect of these two agents on platelet adhesion to fibrinogen regions on the microchannel. ADP and LA were added together to CFSE-labeled PRP according to the protocol described in the Chapter 3.6. ADP concentrations were 0, 2, 5, and 10 μ M, while L-Arginine concentrations were 0, 5, 10 and 15 μ M.

Figure 4-18 shows overall adhesion on the microchannel for all combined concentrations of ADP and LA. Each experiment, with each combination of combined concentrations, was repeated at least three times with different blood samples (collected from the same animal on different days). Error bars are the standard deviations for the three experiments. When ADP concentration increased with LA concentration held constant, platelet coverage increased, which indicates that platelets activated by ADP are sufficient to counteract the effect of L-Arginine to increase the degree of adhesion of platelets to fibrinogen. However, when L-Arginine concentration increased with ADP

concentration held constant, PSAC decreased indicating that NO produced from platelets by conversion of L-Arginine was sufficient to counteract the effect of ADP. Hence, these observations support our hypothesis that platelet adhesion depends on the combined effects of ADP and L-A or NO. In the experiments performed here, neither of the agent completely nullified the effect of the other, supporting the hypothesis that platelet derived NO serves as an inhibitor in negative feedback mechanism and ADP as activator in the positive feedback mechanism of platelets.

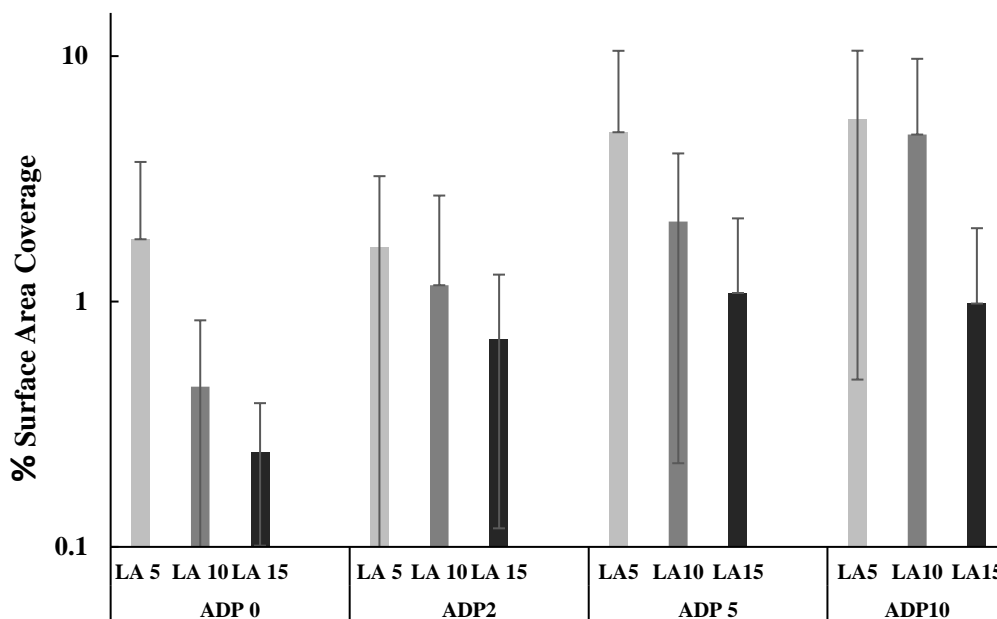


Figure 4-18: Overall platelet adhesion of platelets for all combination of different concentrations of ADP and L-Arginine.

Figure 4-19 shows the PSAC results on the microchannel thrombogenic and non-thrombogenic. For the cases with 0 and 2 μM ADP, PSAC is smaller for T2 than for T1, suggesting that activation at T1 may inhibit adhesion at T2, possibly through the release of NO. For larger ADP concentrations, the pattern was more irregular with respect to fibrinogen region.

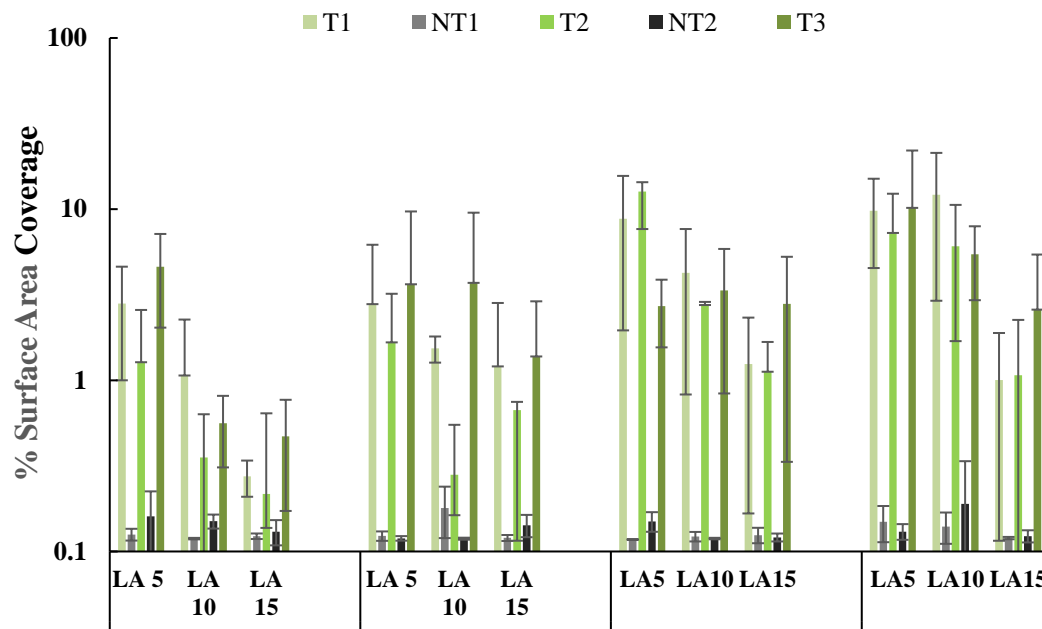


Figure 4-19: Experimental results on effect of percent surface area coverage on combined effect of ADP and LA for different combinations concentrations on microchannel from upstream to downstream say T1-NT1-T2-NT2. Error bars represent standard deviation.

4.6.1 Statistics

The p value of the one factor ANOVA for the overall percent surface area coverage, considering all combinations of ADP and L-A concentrations was 0.0084, indicating that all treatment means are different and the difference among groups is deemed statistically significance for modification of overall platelet adhesion by the combined effect of ADP and L-A.

The p value of the two factor ANOVA for the interaction of combined effect of ADP (2, 5,10 μ M) and L-A (5, 10 and 15 μ M) on different regions of microchannel from upstream to downstream (T1, T2 and T3) is greater than 0.05, it means that F-statistic value is small which tells that there is not much difference in all treatment means and the difference among groups is not statistically significant. The p value for all the conditions

comparing thrombogenic regions is 0.64, indicating no discernable differences in the mean PSAC on the compared thrombogenic regions.

4.7 Combined Effect of ADP- DPTA NONOate on PSAC

DPTA NONOate spontaneously dissociates to generate NO with a half-life of three hours at 37 °C and five hours at 22-25°C, pH 7.4 and can therefore replace deficient levels of NO in patients with CAD. Replacement with exogenous NO donor benefits patients with the impaired activity of the endothelial L-Arginine/NO pathway. DPTA NONOate was added to the CFSE-labeled PRP prior to perfusion into the microchannels. The half-life of DPTA NONOate obscured its combined effect with ADP. The results were paradoxical and not constant throughout the experiments.

Figure 4-20 shows overall adhesion of the microchannel for all combined concentrations of ADP and DPTA NONOate. Each experiment, with each combination of combined concentrations, was repeated at least three times with different blood samples collected from the same animal on different days. Error bars are the standard deviations for three experiments.

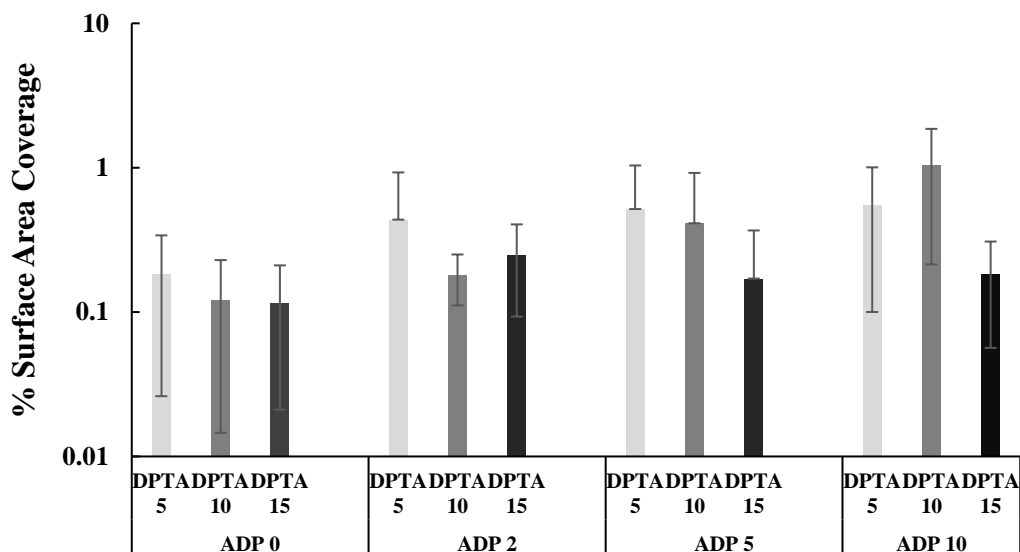


Figure 4-20: Overall platelet adhesion of platelets for all combination of different concentrations of ADP and DPTA NONOate.

When ADP concentration increased with DPTA NONOate concentration held constant, platelet coverage increased, which indicates that platelets activated by ADP are sufficient to counteract the effect of DPTA NONOate and increase the degree of adhesion of platelets to fibrinogen. However, when DPTA NONOate concentration increased with ADP concentration held constant, PSAC decreased, except at ADP 10 μ M concentration, indicating that exogenous NO produced by DPTA NONOate donor and small amount of endogenously developed NO was sufficient to counteract the effect of ADP at lower concentrations but not at higher concentrations. However, ADP was totally neutralized at higher concentration of DPTA NONOate, and platelet adhesion increased as ADP concentration increased. These observations support our hypothesis that platelet adhesion depends on the ratio of ADP to exogenous NO donor, but it suggests that whether platelets are inhibited or activated depends on which agonist has the highest concentration.

Figure 4-21 shows the PSAC results for the five regions on the microchannel. The PSAC values along the channel, from upstream to downstream of thrombogenic regions did not show a consistent pattern with the combined ADP-DPTA NONOate concentrations. Because DPTA NONOate and ADP have different sizes, different diffusion coefficients and different half-life periods, it is reasonable to expect that their transport characteristics will lead to different agonist/antagonist environment at different thrombogenic regions surrounded by non-thrombogenic regions.

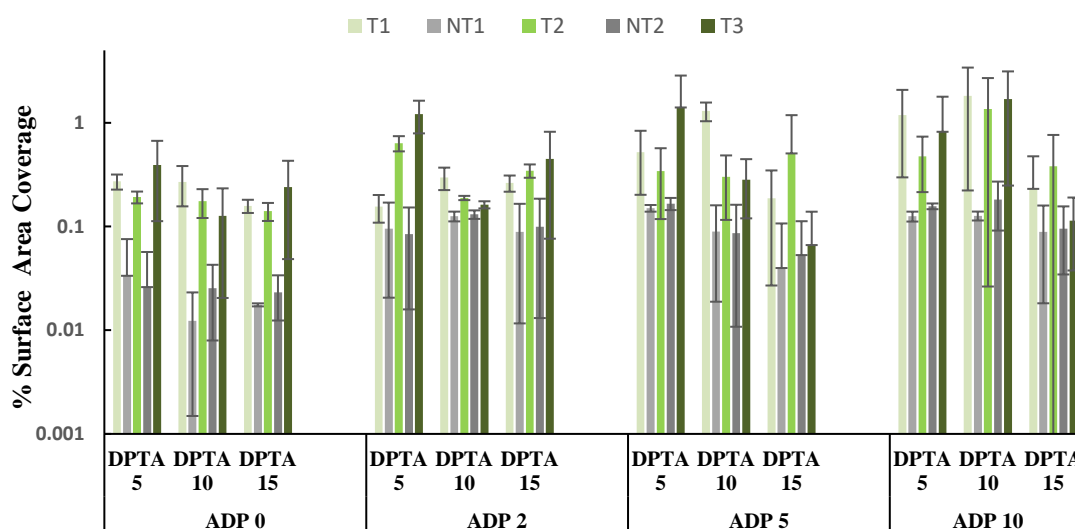


Figure 4-21: Experimental results on effect of percent surface area coverage on combined effect of ADP and DPTA NONOate for different combinations concentrations on microchannel from upstream to downstream say T1-NT1-T2-NT2. Error bars represent standard deviation.

4.7.1 Statistics

The one-way ANOVA test results supports the alternative hypothesis that the difference between the means of overall PSAC for all combinations of ADP (2, 5, and 10 μM) and DPTA NONOate (5, 10, and 15 μM) concentrations with p-value is less than 0.00001, indicating that all treatment means are different and the difference among groups is deemed statistically significance for modification of overall platelet adhesion

by the combined effect of ADP and DPTA NONOate. The two-way ANOVA tests were used to analyze the PSAC for the combined effect of ADP and DPTA NONOate considering all possible combinations of concentrations on thrombogenic regions T1, T2, and T3 along the flow of the microchannel from upstream to downstream. The results support all three null hypotheses because all three p-values are greater than 0.05 indicating no discernable differences in the mean PSAC with combined effect of ADP (2, 5, and 10 μM) and DPTA NONOate (5, 10, and 15 μM) considering all combinations on the compared thrombogenic regions. Percent surface coverage values for these conditions were small and therefore did not have a large enough range with the method used to see a discernable difference between the two factors.

4.8 Calcium Activity in Platelets

4.8.1 Effect of ADP on Calcium Activity in Platelets

Upon stimulation of fluo-4/AM loaded platelets with ADP at different concentrations, we observed a sharp calcium spike followed by another broad spike. Each calcium spike consists of rise and decay phases which was due to change in cytosolic calcium concentration. The spatial and temporal characteristics of calcium spikes envisioned per cell depends on the ADP concentrations. The fluorescence waveforms were monitored and analyzed to determine the changes in calcium peaks with respect to ADP Concentrations (0, 2.5, 5, 10 μM). The calcium peaks obtained were further analyzed to quantify the peak fluorescence intensity that corresponds to peak calcium influx in the cell for all the treatment conditions in the experiment.

Figure 4-22 shows the images of calcium activity in platelets and changes in peak fluorescence intensity before and after stimulating with ADP. Brighter blue colors

indicate calcium influx into the platelet. The signal increases with the addition of ADP, indicating platelet activation, with the secretion of Ca^{2+} into the cytoplasm. The signal is increased to a greater extent with the addition of ionomycin, which increases Ca^{2+} permeability of the sarcoplasmic reticulum and releases Ca^{2+} into the cytoplasm. Thus, ionomycin acts as a positive control to ensure that the calcium indicator functions properly.

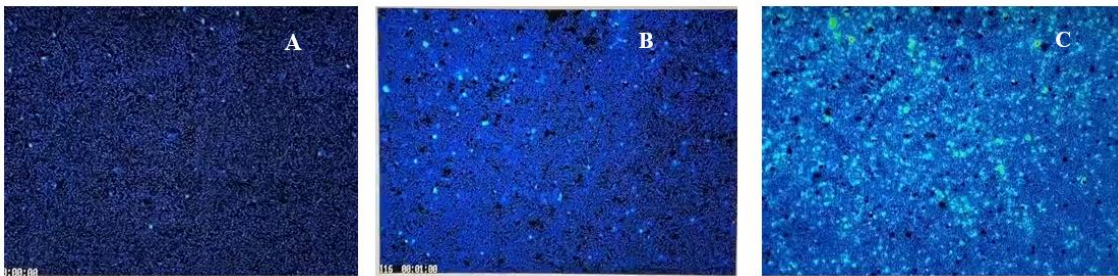


Figure 4-22: Calcium activity in platelets treated with activating stimulus (A) before stimulation (control), (B) after ADP stimulation, and (C) after ionomycin stimulation (positive control).

Fluo-4, single-wavelength indicators are not ideal with the quantitative measurements because of the variations in fluorescence emission may not reflect differences in Ca^{2+} concentration. To correct this uneven indicator concentrations, the fluorescence signal is expressed in relative to its starting signal and is denoted as F/F_0 or $\Delta F/F_0$ where F is the intensity of fluorescence emission recorded during experiment and F_0 is the fluorescence intensity at the start of the experiment.

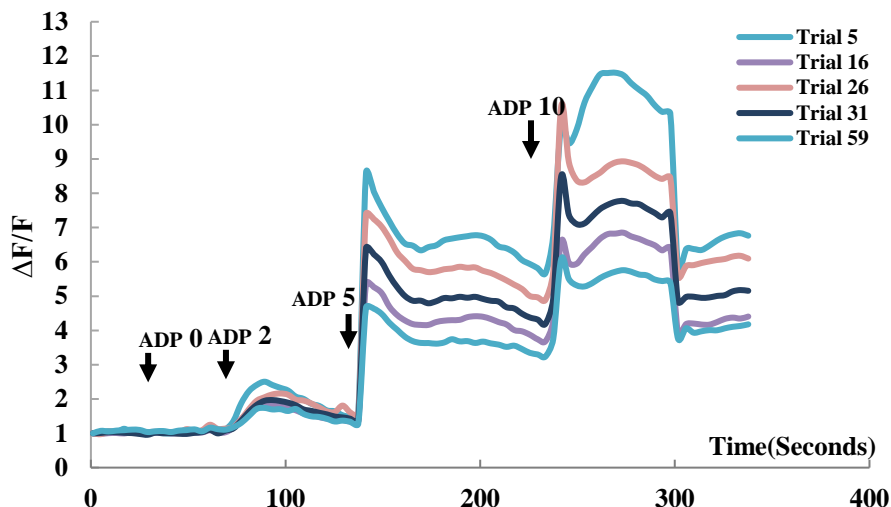


Figure 4-23: Calcium signals recorded for platelets when stimulated with agonists ADP 0,2,5, and 10 μ M concentrations. The X-axis represents frame number and 1 frame = 4 seconds, Y-axis represents normalized fluorescent intensity values.

Figure 4-23 shows the calcium signals recorded for platelets when stimulated with agonists ADP 0,2,5, and 10 μ M concentrations. Trial 5, Trail 16, Trial 26, Trial 31, and Trial 59 are five ROIs selected among 150 to 200 ROIs on average per frame to represent the data obtained for fluorescence intensity over time. The peak fluorescence, showing a response above the normalized fluorescence (1 or 20% above the baseline), after each stimulus increased with increase in ADP concentrations. The higher concentrations of ADP (5 and 10 μ M) caused an immediate rapid increase in $[Ca^{2+}]$, followed by a slower decay phase that represents pumping of Ca^{2+} out of the cytosol. Hence, most of the ADP stimulated platelets with higher concentrations have sharp rise in calcium followed by a decay phase with repetitive transients in calcium.

Analyzing the peak Ca^{2+} fluorescence intensity can be used to support concentration-response relationships for different stimuli and helps in characterizing and measuring the threshold and efficacy of stimulations on cellular responses. The averages of peak

fluorescence intensity for each treatment conditions were calculated, and the values were averaged over 3 experiments.

Figure 4-24 presents the analysis of peak calcium response that corresponds to the normalized fluorescence intensity values above baseline (before stimulation), for platelets stimulated with ADP concentrations 0, 2.5, 5, and 10 μM . Error bars represent the standard deviations. Hence platelets stimulated with ADP showed significant increase in the peak calcium response with increase in its concentrations.

The p value for the one-way ANOVA analyzing different ADP concentrations is 0.04, indicating significant difference in the adhesion characteristics between these conditions.

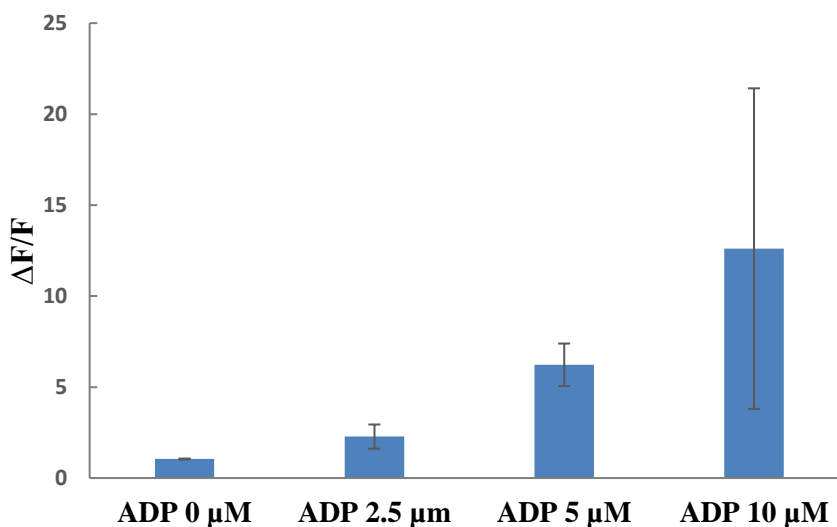


Figure 4-24: Graph showing the peak of the calcium response in platelets stimulated with ADP. Each bar is the averages of $N=3$ experiments with two wells per condition, and with the number of samples (cells) ranging from $n=20$ to 120. Error bars represent standard deviation values.

4.8.2 Combined Effect of ADP and L-Arginine on Calcium Activity in Platelets

The inhibitor L-A (12.5 μM) was added to the ADP-stimulated (12.5 μM) platelets in the wells, and Ca^{2+} spikes were recorded. The intensity of Ca^{2+} peaks

decreased with addition of L-Arginine, with a small dilution artifact followed by a small calcium peak indicating the inhibition effect of NO synthesized by L-Arginine on calcium signaling.

Nitric oxide is powerful inhibitor for agonist-activated platelets and known to decrease calcium concentration in cytoplasm which is elevated by agonists. NO synthesized by L-Arginine by constitutive NO synthase in platelets speeds up the sarco-endoplasmic reticulum Ca^{2+} ATPase (SERCA)-dependent refilling of internal Ca^{2+} stores by decreasing the calcium concentration in cytoplasm and has long been recognized to inhibit platelet activation by increasing the synthesis of cyclic-3'5'-guanosine monophosphate (cGMP) *via* direct stimulation of the enzyme soluble guanylate cyclase (sGC). CGMP activates PKG, which blocks phospholipase C, which in turn blocks IP3 and decreases the intracellular calcium concentrations.

The fluorescence waveforms were monitored and analyzed to determine the changes in calcium peaks in ADP stimulated platelets with respect to L-Arginine. The data obtained for fluorescence intensity over time for each ROI were then normalized to their starting values (baseline) in Microsoft Excel, for obtaining correlation between cells within an experiment and with other experiments. The normalized values of fluorescence intensity over time are represented using line graphs.

Figure 4-25 shows the normalized values of fluorescence over time for ADP stimulated platelets and the effect of L-Arginine on them. The graph indicates significantly inhibited Ca^{2+} response with the addition of L-A after stimulating platelets with ADP to see the combined effect of ADP-LA on calcium activity. These findings support the *in vivo* behavior of platelets depend on its calcium activity, where with low

[Ca²⁺] indicates the secretion of inhibitor such as NO and high [Ca²⁺] levels indicate secretion of activation agonists such as ADP. Trial 8, Trial 17, Trial 30, Trial 45, and Trial 48 are five ROIs selected among 150 to 200 ROIs on average per frame to represent the data obtained for fluorescence intensity over time.

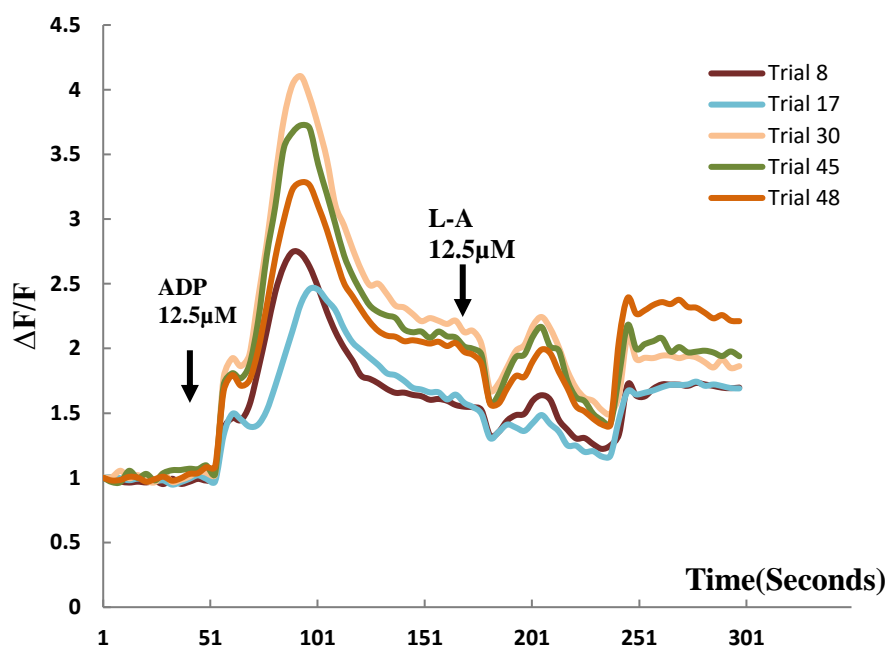


Figure 4-25: Calcium signals recorded for the ADP of 12.5 μM stimulated platelets with the addition of L-A 12.5 μM . The X-axis represents frame number and 1 frame = 4 seconds, Y-axis represents normalized fluorescent intensity values.

Measuring and analyzing the peak Ca²⁺ fluorescence intensity helps in providing concentration-response relationships for different stimuli. The calcium peaks obtained were further analyzed to quantify the peak fluorescence intensity that corresponds to peak calcium influx in the cell for all the treatment conditions in the experiment.

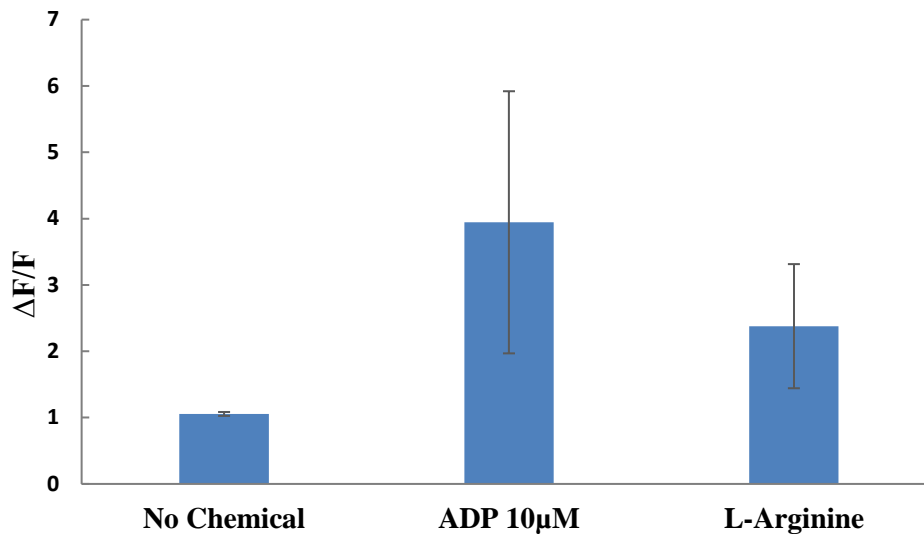


Figure 4-26: Graph showing results for peak calcium response after L-A is added to platelets stimulated with ADP to the normalized fluorescence intensities. Data represent the averages of N=3 experiments with two wells per condition, and no. of samples (cells) ranging from n= 20 to 120. Error bars represent standard deviation values.

Figure 4-26 shows the analysis of peak calcium response of ADP stimulated platelets with addition of L-A. The data represents an average of 3 experiments and error bar represents the standard deviations. Hence, addition of L-A to the ADP stimulated platelets showed significant decrease in the peak calcium response by inhibiting the intracellular $[Ca^{2+}]$. The one-way ANOVA test for the fluorescent peak for different stimulus on platelets yielded a p value of 0.01 indicating a statistically significant effect at the $\alpha=0.05$ level.

4.8.3 Effect of ADP-DPTA NONOate on Calcium Activity

The platelets release the calcium from all the intracellular calcium stores upon stimulus with ADP into cytoplasm. This process increases the cytoplasmic calcium concentrations. The calcium released in the cytosol is either actively taken up by the ER via calcium channels called Sarco-Endoplasmic reticulum Ca^{2+} -ATPase (SERCA) or it is flushed out through calcium channels present in plasma membrane. When DPTA

NONOate, an exogenous NO donor, was added to ADP stimulated platelets, it decomposes itself in PBS and activates Sarco-Endoplasmic reticulum Ca^{2+} -ATPase (SERCA) by decreasing the elevated calcium concentrations in ADP stimulated platelets.

The intensity of Ca^{2+} peaks were high with the addition of ADP and went low with addition of NO donor, DPTA NONO when compared with the calcium peaks of ADP stimulated platelets.

Figure 4-27 shows the normalized values of fluorescence over time for ADP stimulated platelets and the effect of DPTA NONOate on them. Trial 56, Trail 74, Trial 81, Trial 96, and Trial 151 are five ROIs selected among 150 to 200 ROIs on average per frame to represent the data obtained for fluorescence intensity over time. The elevations of calcium spikes in ADP stimulated platelets before adding NO donors might vary in between platelets or in between experiments due the physiological conditions of blood and its behavior on different days.

The graph indicates significantly inhibited Ca^{2+} response with the addition of DPTA NONOate after stimulating platelets with ADP to see the combined effect of ADP-DPTA NONOate on calcium activity. These findings are consistent with the inhibiting property of NO and shows that it leads to a reduction in intracellular $[\text{Ca}^{2+}]$. The inhibition effect of DPTA NONOate on the elevated levels of calcium peaks in ADP stimulated platelets is not much effective when compared with inhibition effect of L-A on ADP stimulated platelets. The unstable nature of DPTNA NONOate, its short half-life, and the ability of NO that can react with superoxide (O_2^-) forming peroxy-nitrite (ONOO^-) were it exhibits both inhibitory and excitatory effects in platelets are few factors which limits the inhibition rate of DPTA NONOate.

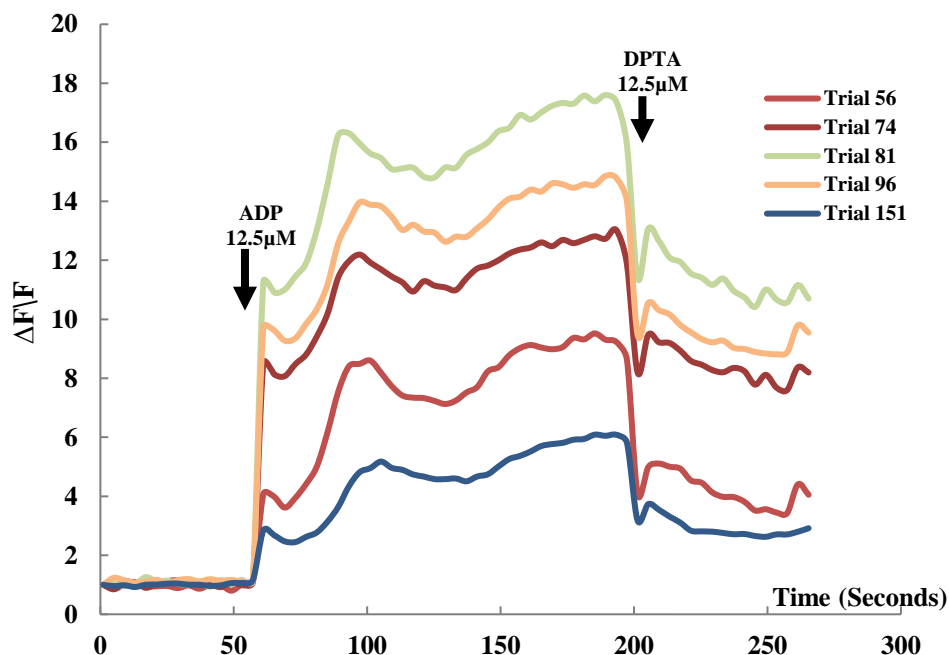


Figure 4-27: Calcium signals recorded when DPTA NONOate is added to ADP-stimulated platelets. The X-axis represents frame number and 1 frame = 4 seconds, Y-axis represents normalized fluorescent intensity values.

Figure 4-28 shows the analysis of peak calcium response of ADP stimulated platelets with addition of DPTA NONOate. The data represents an average of 3 experiments and error bar represents the standard deviations. The effect of DPTA NONOate to the ADP stimulated platelets showed significant decrease in the peak calcium response by inhibiting the intracellular $[Ca^{2+}]$. The one-way ANOVA test for the peak fluorescent intensities for different stimulus on platelets yielded a p value of 0.03 indicating a statistically significant effect at the $\alpha=0.05$ level.

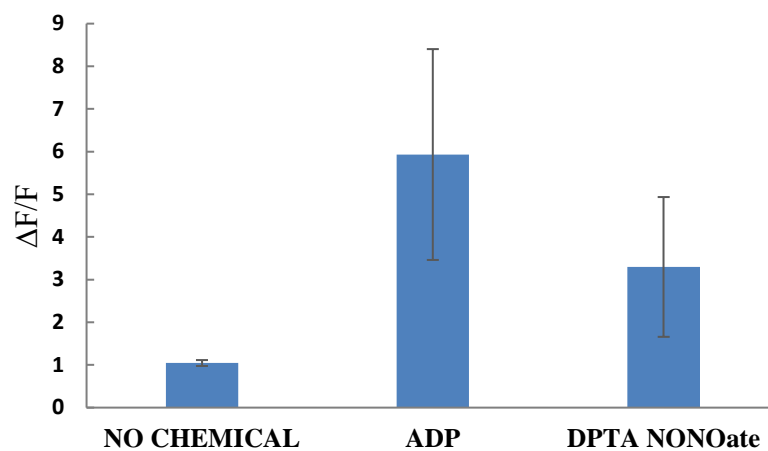


Figure 4-28: Peak calcium response of DPTA NONOate on platelets stimulated with ADP to the normalized fluorescence intensities. Data represent the averages of N=3 experiments with two wells per condition, and no. of samples (cells) ranging from n= 20 to 120. Error bars represent standard deviation values.

CHAPTER 5

DISCUSSION

A micro channel patterned with thrombogenic regions (coated with fibrinogen) and non-thrombogenic region (coated with BSA) was created and used to study simultaneous positive and negative feedback effects on regions in which thrombus formation is active next to regions in which thrombus is prevented.

Many models which are being developed for platelet-mediated thrombo-genesis considered the effects of platelet activators and inhibitors separately, but our microchannel model helped us to study the combined effects of platelet derived activators (ADP) and inhibitors (endogenous and exogenous NO donors) in one region influencing platelets in a different region under varying shear conditions. The individual agents ADP, L-Arginine, and DPTA-NONOate will be added to the PRP prior to injection through the channels, and the amount of adhesion will be quantified as a function of the concentration of each agent.

Agents like ADP and NO produced or released by activated platelets acts as paracrine signaling molecules in activating other platelets in developing thrombus formation. The signaling within a growing thrombus and signaling between two different thrombi both are paracrine signaling but their effects differ depending on the agents released and their concentrations, and agents released in one thrombogenic region influencing the platelets on other thrombogenic region.

5.1 Effect of ADP Concentrations on PSAC

ADP is a well-known activator that enhances contact-induced activation of platelets. However, it was important to demonstrate that agents such as ADP released by platelets in a growing thrombus affect the growth of thrombus downstream. Multiple thrombogenic surfaces arranged in the streamwise direction can help to verify this hypothesis. The base slide consisted of thrombogenic regions (labeled T1, T2, and T3 from upstream to downstream) coated with fibrinogen from upstream to downstream. These regions were separated by non-thrombogenic regions (NT1 and NT2) coated with BSA. The base slides were perfused with CFSE-labeled platelets with different concentrations of ADP (0, 2, 5, and 10 μM) at a shear rate 1500 s^{-1} , and MATLAB was used to calculate the PSAC from the fluorescent images.

Overall PSAC of the microchannel increased as ADP concentration increased, and again the effect was dose dependent from **Figure 4-10**. High exogenous ADP concentration (10 μM) on thrombogenic regions T1, T2, and T3 increased PSAC from upstream to downstream because the endogenous and released ADP after platelets activation overwhelmed the production of NO flowing from upstream to downstream. Lower ADP concentrations (2 and 5 μM) increased PSAC at T1 and T2, but decreased PSAC at T3, indicating that ADP at T1 would activate the platelets, causing them to release more ADP which leads to increase PSAC at T2, but that NO produced at T1 and T2 would flow downstream and inhibit PSAC at T3.

One-way and two-way ANOVA tests supported the alternative hypothesis overall PSAC for the three concentration of ADP 2, 5, and 10 μM differ. They also supported that the means of PSAC on different thrombogenic regions (T1, T2, and T3) differ.

The P values for the one-way ANOVA test was 0.000315 and the p-values for two-way ANOVA with three null hypothesis were 0.002, 0.000000426, and 0.03 which is less than the $\alpha = 0.05$ hence null hypotheses were rejected. This p value suggested a significant difference in the adhesion characteristics among ADP concentrations with different locations of thrombogenic regions.

5.2 Effect of L-Arginine on PSAC

NO inhibits the activation of platelets and prevents recruitment of additional platelets to the platelet plug. The high diffusion coefficient of NO, a consequence of its small size, has a significant role in inhibiting activated platelets. Experiments were performed to determine whether the addition of L-Arginine, the precursor of NO, would reduce the PSAC on the microchannel with thrombogenic and non-thrombogenic regions. The images demonstrated reduced adhesion with increased L-Arginine qualitatively, and the quantitative MATLAB analysis of these images demonstrated that the effect was dose-dependent and repeatable.

The quantitative analysis states that overall PSAC of the microchannel decreases with increased L-Arginine concentrations. The PSAC on the microchannel for different concentrations of L-Arginine on different locations of thrombogenic regions T1, T2, and T3 were small and therefore did not have a large enough range with the method used to see a discernable difference between the two conditions. No significant results were observed when comparing PSAC of T1, T2, and T3 with addition of L-A (5, 10, and 15 μM) concentrations. The one-way ANOVA and two-way ANOVA tests results supported only the alternative hypothesis that the means of overall PSAC for three

concentration of L-A 5, 10, and 15 μM are not same. The other hypotheses were rejected ($p > 0.05$).

5.3 Effect of DPTA NONOate on PSAC

DPTA NONOate is the most available exogenous NO donor. The high diffusion coefficient of NO enhances its transport to platelets, potentially enhancing its effect.

DPTA NONOate spontaneously releases NO with a half-life of three hours at 37 °C and five hours at 22-25 °C, pH 7.4. Experiments were performed to determine whether the addition exogenous NO donors modulated the bioactivity of endogenously produced NO in platelets and whether the consequent increased NO levels reduce the PSAC on the microchannel.

DPTA NONOate was added to the CFSE-labeled PRP prior to perfusion into the microchannels. The overall PSAC initially decreased for lower concentrations of DPTA NONOate (5 μM) and maintained a constant level at higher concentrations (15 and 20 μM). Though DPTA NONOate at higher concentrations did not continue to decrease the overall PSAC significantly, PSAC did not exceed the levels of the control and maintained a constant role in inhibiting the activated platelets.

The inhibition effect of DPTA NONOate on the microchannel was not same when compared with inhibition effect of L-A, possibly because of difference in their mechanism of action on platelets from upstream to downstream. DPTA NONOate, which does not require the action of the platelets to produce NO whereas L-Arginine is a precursor that stimulates production of NO by platelets. These different mechanisms of NO production by L-Arginine and DPTA NONOate might affect the difference in PSAC from upstream to downstream regions (T1-T2-T3). In the case of endogenous NO donor,

L-Arginine, it stimulates NO in T1, and convection of that NO may inhibit thrombus on T2, but not on T1, whereas DPTA NONOate, would possibly affect T1 and T2 by the same amount due to exogenous production of NO is almost same on both the regions T1 and T2. This might be one of the reason where the mean PSAC values of T1 > T2 with addition of L-Arginine for three different concentrations have different effect on thrombogenic regions, though not statistically significant, in comparison to the DPTA results where the mean PSAC values of T1 \approx T2 are intriguing.

The one-way ANOVA and two-way ANOVA tests results supported only the alternative hypothesis that the difference between the means of overall PSAC for three different concentration of DPTA NONOate 5, 10, and 15 μ M are not same. All other alternative hypotheses were rejected ($p > 0.05$).

5.4 Combined Effect of ADP with Exogenous and Endogenous NO donors on PSAC

The primary interest of this study is the combined effect of activator (ADP) and inhibitor (NO) on platelet activation, adhesion, and recruitment. Both agents are present in different amounts in any in vivo environment with absolute and relative concentrations varying spatially because of local differences in their production and transport (both diffusional and convective). The combination of both agents was added to CFSE-labelled PRP prior to perfusion at different concentrations into microchannel.

5.4.1 Combined Effect of ADP-L-A on PSAC

With LA concentration held constant and ADP concentration increasing, the overall PSAC increased, which indicates that ADP activation is still dose-dependent with this baseline level of L-Arginine. Similarly, with ADP concentration held constant and

L-Arginine concentration increasing, the overall PSAC decreased indicating that NO produced from platelets by conversion of L-Arginine is still dose-dependent with this level of ADP. Hence, these observations support our hypothesis that platelet adhesion depends on the combined effects of ADP and L-A or NO and that neither agent completely erases the effect of the other. These results are consistent with a model in which ADP is an activator in the positive feedback mechanism of platelet activation that is modulated by a negative feedback loop that involves NO.

The one-way ANOVA test results supports the alternative hypothesis that the means of overall PSAC for all combinations of ADP (2, 5, and 10 μM) and L-A (5, 10, and 15 μM) vary, with p-value 0.0084.

Because L-A and ADP have different sizes and hence different diffusion coefficients, it is reasonable to expect that their transport characteristics will lead to different agonist/inhibitor environments at different regions within and near the thrombus. However, different amounts of adhesion between upstream, middle, and downstream thrombogenic regions did not show a clear pattern in studies on the combined effect of ADP and L-A. The two-way ANOVA tests results rejected all three null hypotheses ($p > 0.05$). While further studies need to be carried out, to determine what affect transport may have on the growth and the control of thrombus growth.

5.4.2 Combined Effect of ADP- DPTA NONOate on PSAC

When DPTA NONOate concentration was held constant while ADP concentration was increased, platelet coverage increased. Thus, ADP acts in a dose-dependent manner at the constant level of DPTA NONOate. Similarly, when ADP concentration was held constant while DPTA NONOate concentration increased, PSAC

decreased, except at ADP 10 μM concentration, indicating that, in general, neither agent negated the effect of the other but that the high ADP level was sufficient to negate the effect of DPTA at the concentrations used. These observations support our hypothesis that platelet adhesion depends on the relative concentrations of ADP and NO donor.

The one-way ANOVA test result supports the alternative hypothesis that overall PSAC varies for all combinations of ADP (2, 5, and 10 μM) and DPTA NONOate (5, 10, and 15 μM) concentrations ($p < 0.00001$). Two-way ANOVA tests were used to analyze the PSAC for the combined effect of ADP and DPTA NONOate, considering all possible combinations of concentrations on thrombogenic regions T1, T2, and T3 along the flow direction of the microchannel. The results support the null hypothesis for all three regions ($p > 0.05$). Percent surface coverage values for these conditions were small and may not have had sufficient range, with the method used, to discern differences between the two factors.

5.5 Effect of ADP, L-A, and DPTA NONOate on Calcium Signaling

Platelet derived activators (ADP) and inhibitors (NO) not only effect the thrombus formation but also increases the cytosolic calcium concentration of platelets when activated. Activation and inhibition pathways of platelets trigger calcium stores in platelets at site of thrombus formation. Increase or decrease in cytosolic Ca^{2+} concentration plays a crucial role in platelet activation and could lead to accelerated thrombus growth or decelerated thrombus growth, depending on whether the activators or the inhibitors from the upstream thrombus are more dominant.

Platelet agonists release Ca^{2+} from intracellular stores during platelet activation plays a crucial role in regulating many platelet functions. Increase in calcium

concentration in platelets are due to the release of Ca^{2+} from compartments and entry of extracellular Ca^{2+} through plasma membrane. Calcium signaling in activated platelets through agonists acts as paracrine signals. These signals usually produce quick responses which lasts for only short time. The interplay between positive and negative feedback with respect to calcium signaling is largely unknown. We evaluated calcium release in vitro at single cell level in free moving cells, while neglecting the effect of NO release in inhibiting calcium concentrations. Platelet poor plasma was loaded with Fluo-4 Ca^{2+} ion indicators, and the fluorescence waveform was measured and analyzed after addition of ADP and NO donors (exogenous and endogenous). Most of the experiments demonstrated an agonist-induced platelet activation that involved a sharp increase in intracellular calcium ions [68][69].

Calcium response increased with increased ADP concentrations (0, 2.5, 5, 12.5 μM) and had a greater number of significant calcium oscillations when compared to calcium response produced with addition of L-A/DPTA NONOate. A significant decrease in calcium response was observed with these latter two agents.

5.6 Effects of Shear Rates

Shear rate is one of the main factor that affect the processes that control the rate of thrombus formation [70]. The higher shear rates from 1000 – 10,000 s^{-1} were found in atherosclerotic lesions, preexisting thrombi, regions of moderate arterial stenosis and platelet-platelet interactions which results in prothrombotic microenvironment [71][72]. The base slide of the microchannel was coated with fibrinogen to produce a thrombogenic surface and evaluated platelet adhesion at a shear rate of 1500 s^{-1} representing the shear rate different conditions of adding no chemicals and varying

amounts of ADP, L-A and DPTA NONOate. Due to the time limitations, we were unable to run few more set of experiments at different shear rate and unable to evaluate the effect of shear rate on these hypotheses.

There were no direct comparisons found for the method used in this work all through the literature at shear rate 1500 s^{-1} to compare the results of combined effects of LA-ADP/DPTA NONOate on platelet adhesion. Sanakam and Adams results showed that L-A added to PRP saw an overall increase in adhesion at 1500 s^{-1} compared a lower shear rate of 500 s^{-1} for the microchannel with thrombogenic region size of 6mm X 6mm and 8mm X 8mm coated with fibrinogen, which did not agree with the results of Watson's method where he used a fibrinogen coating to investigate the effect of shear rates and saw a reduction in overall adhesion at higher shear rates with addition of L-A [33][34][62]. Our results by using the similar method as Sanakam and Adams did, but with thrombogenic regions of size 2mmX2mm coated with fibrinogen for different concentrations of L-A and DPTA NONOate, showed reduction in platelet adhesion in agreement with the results of Watson's method [62]. The results for the combined effect of ADP- L-A/ ADP- DPTA NONOate on platelet adhesion at different thrombogenic regions for different concentrations of L-A/ADP/DPTA NONOate were inconclusive and shear rate might be one of the reason altering the effect of T1 on T2 and T2 on T3.

5.7 Comparison of Results to Other Sources

Sihui Xu and his team developed a microfluidic device to study platelet adhesion and aggregation under shear flow pathophysiological conditions. Platelet activation in upstream was performed either by using agonists or by shear flow and platelet adhesion in downstream was caused by collagen-coated microbeads loaded in tube [73]. Their

results showed that platelet adhesion in downstream was dependent on platelet activation in upstream including parameters like shear rate ($754\text{-}2400\text{ s}^{-1}$), shearing time ($>10\text{ s}$), and incubation time ($>20\text{ s}$). They also produced real-time of platelet related thrombus formation by combining a variety of leading-edge technical elements. The portion of their results agreed with the results of our work were the effect of platelet adhesion on the downstream region with the addition of chemical agents depends on platelet activation in upstream regions and agents released by platelets.

Shekh Rahman and Vladimir Hlady developed a microfluidic system consists of flow channel with upstream stenotic region and downstream protein capture region to perfuse whole blood and used to evaluate the effect of antiplatelet agents inhibiting platelet adhesion under shear flow. Platelet binding proteins like collagen, fibrinogen and vWf were patterned using microcontact printing on the surface of downstream capture region. Whole blood with antiplatelet agent was perfused through upstream region under shear rate ranging from $4860\text{ to }11560\text{ s}^{-1}$. Their results showed that Acetylsalicylic acid failed in inhibiting shear-induced platelet adhesion to all three binding proteins whereas GPIIb/IIIa inhibitors (tirofiban and eptifibatide) significantly inhibited platelet adhesion to fibrinogen. Platelet adhesion reduced with all three capture proteins by blocking antibody of vWf or GPIIb [74]. The portion of their hypothesis evaluating the effect of platelet adhesion for different group of antiplatelet agents like GPIIb/IIIa inhibitors under shear flow conditions was almost similar to our hypothesis where platelet adhesion decreases with the addition of NO inhibitors under the influence of shear rate 1500 s^{-1} on a microchannel with thrombogenic regions coated with fibrinogen.

Avtaeva and his team introduced a testing system for real time recording of the platelet kinetics adhered to fibrinogen-coated surface under flow conditions. Their system consists of an optical flow chamber, semiconductor laser, two photodetectors, analog to digital converter, computer, and peristaltic pump. Photodetectors were used to record the platelet adhesion to fibrinogen coated optical surface and analyzed the intensity of total internal reflection and scattered laser radiation [75]. A function of shear rate and platelet concentration was used to study the platelet adhesion kinetics and its specificity was verified by blocking IIb/IIIa glycoprotein complex on platelets by using Fab2 fragments of monoclonal antibodies. These results by their testing system show that kinetics of adhesion of ADP-activated platelets to protein-coated surface under controlled flow conditions were recorded effectively and were in accordance with the results of effect of ADP on platelet adhesion on microchannel coated with fibrinogen.

J.E. Freedman's study said that NO when released by platelets inhibits further recruitment of platelets forming a thrombus. The thrombotic response can be altered by modulating endogenous platelets and regulate several clinical diseases with low NO bioactivity and bioavailability, by replacing with exogenous NO donors [16][76][77][78]. This result agrees with the results of this work. L-A that produced by oxidizing constitutive nitric oxide synthase (cNOS) was used in this work and observed the results that reduced platelet activation and recruitment. The results of these experiments agreed with the results of our work where with the addition of L-A decreases the overall PSAC of platelets adhered to the microchannel.

A procedure demonstrated by Bellavite and his colleague through a colorimetric method for the measurement of platelet adhesion in microtiter plates by ADP and

thrombin stimulated platelet adhesion in dose dependent manner to fibrinogen but not to albumin [68]. The results determined in these experiments agreed with the results of our work where the overall PSAC of the microchannel increased in dose dependent manner with effect of ADP.

A study done at University of Oklahoma and Baptist Medical Center located in Oklahoma explained the link between the region space and platelet aggregation where the method used for this investigation was different from the method used our work with isolated thrombogenic regions as opposed to lines across the slide or down the slide used for thrombogenic regions. This work was done at a lower shear rate of 100 s^{-1} in contrast to our work at higher shear rates of 500 s^{-1} and 1500 s^{-1} and results were inconclusive when compared [69].

5.8 Sources of Experimental Errors

The experiments were lengthy, and because platelet function can change rapidly after blood is removed from the host, most of the process had to be done in one day. This requirement limited the number of trials that could be done for a given condition. The main sources of error in these experiments were time delay.

Some manual errors may occur while pasting Kapton tape on the slide in the right position, while sandwiching the tape and glass slide consistently each time manufacturing the microchannel. The accuracy in Kapton tape cutting in desired shape and size and accuracy in drilling the inlet and outlet holes depends on the cutters machine and driller machines precision respectively.

5.9 Variability in Experiments

Patterning of thrombogenic regions with fibrinogen manually should be consistent and accurate along the channel to see the change in PSAC on different thrombogenic regions. A method which provides higher accuracy values for patterning proteins should be developed. The thickness of the fibrinogen and BSA layers should also be quantified using X-ray reflectivity (XRR) and atomic force microscopy (AFM) methods [79]. Consistent variability along the channel, or from region to region, could affect the amount of adhesion, and thus the interpretation of the results.

Systematic investigation was needed to determine the optimal flow rates for rinsing and drying to avoid droplets and debris at imaging stage. Insufficient rinsing and drying leads to artifacts in the imaging.

The samples of bovine blood collected from Tech Farms needed to be properly mixed with anticoagulant to avoid the blood clots and then used in the same day. The platelets extraction from blood is recommended within first two hours. The physiological conditions of blood can differ with samples each day, even though the samples were from same source and hence expected some variability in platelets count [80] [81].

DPTA NONOate is the most available exogenous NO donor with high diffusion coefficient of NO and consequence of its small size has a significant role in inhibiting activated platelets. DPTA NONOate spontaneously dissociates NO with a half-life of three hours at 37°C and five hours at 22-25°C, pH 7.4. DPTA NONOate, when not used before its half-life period expires, will exhibit a substantial reduction in its inhibition effect. For a given NO donor, DPTA NONOate with a half-life of 5 hours, the initial NO concentration will be approximately 0.54×10^{-3} times the initial donor concentration

(millimolar concentrations of donor yield nanomolar concentrations of NO. The expected concentration of NO, for the given the concentrations of 5, 10, and 15 μ M DPTA NONOate were 2.7, 5.4, and 8.1nM respectively which were greater than the minimum NO concentration required to inhibit platelets under all conditions that is 0.15nM [66].

CHAPTER 6

CONCLUSIONS AND FUTURE WORK

6.1 Conclusions

The results from the microchannel experiments suggest the following conclusions.

- Percent surface area coverage of platelets will increase dose-dependently when platelet derived activators (e.g., ADP) are included and decrease dose-dependently when NO donors (L-A and DPTA NONOate) are included in the perfused plasma.
- Adhesion increased when L-Arginine concentration was held constant and ADP concentration was increased. Furthermore, when ADP concentration was increased and L-Arginine concentration was held constant, platelet adhesion decreased. Neither ADP nor NO was completely neutralized by the other agent at any of the concentrations used in this study.
- For a fixed amount of DPTA-NONOate added to the PRP, platelet surface area coverage increased with increased plasma ADP concentration. Likewise, for a fixed amount of ADP added to the plasma, platelet surface area coverage decreased with increased DPTA-NONOate concentration.
- Calcium response in plasma free platelets loaded with the fluorescent Ca^{2+} indicator Fluo-4 increased dose-dependently with addition of an activator, ADP.

- Calcium response in ADP stimulated platelets decreases with addition of L-A indicating the immediate inhibition effect of NO synthase endogenously in ADP stimulated platelets.
- Addition of exogenous NO donor DPTA-NONOate, with the intent to overwhelm the endogenous feedback through platelet NO production, decreased $[Ca^{2+}]$ peaks.

6.2 Future Work

6.2.1 Platelets Count

Platelet count was not quantified in these studies. Although the blood samples are from the same source, we expected variability in platelet count from sample to sample. Counting platelets before experiments might improve statistical analysis and decrease the variability in results. Testing platelet samples independently in an aggregometer before each experiment to determine the changes in platelet activity in each sample and correlate it to the behavior of the microchannel under flow would give better results.

6.2.2 Patterning of Proteins Using Nano eNabler

Patterning proteins like fibrinogen or collagen on thrombogenic regions of size 2 mm by 2 mm manually is very hard to be precise, accurate and repeatable. The Nano Enabler is the tool used to lay proteins in minute volumes of liquid at specified positions as designed with high spatial accuracy by reducing clogging. Experiments preparing the base slide of the microchannel this way would give the ability to do more complicated experiments. All conditions evaluated in this dissertation would need to be repeated using this modification to the method.

6.2.3 Effect of Proteins on Platelet Adhesion

Proteins like fibrinogen and collagen play a key role in thrombus formation and are considered as important ligands for platelet adhesion to artificial surfaces. The time limit and the need for blood samples to be used on same day, prevented experiments for microchannel patterned with collagen on thrombogenic regions and examine their effect on platelet adhesion. All conditions evaluated in this dissertation would need to be repeated using this modification to the method.

6.2.4 Real-Time Analysis

Real-time analysis would benefit the platelet adhesion study because we could closely monitor the platelets adhering to thrombogenic and non-thrombogenic regions and effect of activators and inhibitors on it. The system can be modified to allow visualization of the surface during the flow experiment with a video camera.

6.2.5 Combined Effect of ADP- DPTA NONOate on PSAC

All the calcium signaling experiments in this dissertation were done using 96 well flat plates with high affinity were recorded. The experiments were then analyzed in InCyt Im™ Imaging System software in real-time. Additional information could be obtained if a method were devised to examine calcium signaling in platelets with addition of exogenous and endogenous agents on microchannel with thrombogenic patterned with fibrinogen or collagen and non-thrombogenic regions blocked BSA under different shear rates with InCyt Im™ Imaging System software in real-time.

6.3 Future Applications

The model used here is not only translatable to cardiovascular diseases like atherosclerosis with more irregular and frequently diffuse pattern of platelet adhesion and

thrombosis, but the findings may also extend to stent development. The methods used in dissertation can be further used to assess the efficacy of anti-platelet treatments of a stent that has multiple thrombogenic and non-thrombogenic regions with platelet recruitment.

These methods are useful while designing stents which were coated with anti-platelet drugs for example a stent that is coated with a Nitric Oxide (NO) donor could have multiple separated regions of NO release and thrombogenic tissue, will greatly diminish the thrombus that forms on stents and consequently reduce complications of occlusive thrombosis and intimal hyperplasia.

APPENDIX A

PROGRAM USED TO CALCULATE PSAC

```
% Collect the names of all subdirectories in "folders."
thresh = 30;
files = dir('E*');
dirflags = [files.isdir];
directories = files(dirflags);
% Create an Excel file that contains the percent coverage values for
all
%files.
w = what;
mypath = w.path;
xlsfilename = [mypath '\\' 'Percentages.xls'];
ExcelFileLine = 1;
% Print folder names to command window.
for k = 1 : length(directories)
    folder = directories(k).name;
    Subfoldername = {folder};
    fprintf('Sub folder #%d = %s\n', k, folder);
    thecell = sprintf('A%d',ExcelFileLine);
    ExcelFileLine = ExcelFileLine + 1;
    [stat msg] =
xlswrite(xlsfilename,Subfoldername,'Percentages',thecell)
    [pct ExcelFileLine] = doimg(folder,thresh, ExcelFileLine,
xlsfilename);
    ExcelFileLine = ExcelFileLine + 1;
end

function [pct LineNo] = doimg(foldername,thresh,ExcelFileLine,
xlsfilename)
% Process and image
% Get the name of the folder in which the images are kept.
% ***** Change this name for different directories
% foldername = 'E1S1R1C2L-NMMA';

% Change the threshold, if necessary. It should have a value between 0
and
% 255.
thresh = 30.

% Get the screen heigh and width (to place the plots on the screen).
scrsz = get(0,'ScreenSize');
wid = scrsz(3);
```

```

hgt = scrsz(4);

% Find the current working directory (so that you can find the image
file
% name).
w = what;
mypath = w.path;

imgs = [foldername '/' '*.tif']; % Full path of the folder where the
images are kept.

% Create a list of all image files in the image folder.
allimgs = dir(imgs);

% Find out how many image files are in that folder.
s = size(allimgs);
Ntotal = s(1);

% For each file in the folder, process the image.
f1 = figure(1);
f2 = figure(2);
for i = 1:Ntotal
    fullfilename = [foldername '\' allimgs(i).name]; % Full path name
of the file.

% Read the image into MATLAB as an array I.
I=imread(fullfilename);

% Uncomment the next three lines if you want MATLAB to show the original
image.
% Title = ['Original ' allimgs(i).name]
% figure('Name', ['Original ' allimgs(i).name], 'Position', [wid/10
hgt/1.8 wid/3 hgt/3]);
% image(I);

% Resize the image to a more managable heigh and width.
Ismall = imresize(I,384,512);
close(f1);
close(f2);
f1 = figure('Name', ['Small ' allimgs(i).name], 'Position', [5*wid/10
hgt/1.8 wid/3 hgt/3]);
image(Ismall);

% The Mex file threshold.mex changes the image to grayscale and then
sets
% all pixels greaterh than thresh to 255 and all pixels less than
thresh to
% 0.
[Ithresh pct] = threshold(Ismall,thresh);

% Subtract 0.1770 from the percent coverage. This is the percent of
the
% image that is covered by the length scale label. It would be better
to
% account for the label in some other way, but we will go with this for

```

```
% now.
    pct = pct - .1770;

% Show the thresholded figure
    f2 = figure('Name', ['Threshold '
allings(i).name], 'Position', [5*wid/10 hgt/10 wid/3 hgt/3]);
    imshow(Ithresh);

% Write the percentage data to the Excel file.
    thename = {allings(i).name, pct};
    thecell = sprintf('A%d', ExcelFileLine);
    [stat msg] = xlswrite(xlsfilename, thename, 'Percentages', thecell)
    ExcelFileLine = ExcelFileLine + 1;

    LineNo = ExcelFileLine;

    % Uncomment the next line to clear all figures
%close all
```

BIBLIOGRAPHY

- [1] J. Frostegård, “Immunity, atherosclerosis and cardiovascular disease,” *BMC medicine*, vol. 11, no. 1, pp. 1–13, 2013.
- [2] F. Sanchis-Gomar, C. Perez-Quilis, R. Leischik, and A. Lucia, “Epidemiology of coronary heart disease and acute coronary syndrome,” *Annals of translational medicine*, vol. 4, no. 13, p. 256, 2016.
- [3] L. Badimon, T. Padró, and G. Vilahur, “Atherosclerosis, platelets and thrombosis in acute ischaemic heart disease,” *European heart journal: acute cardiovascular care*, vol. 1, no. 1, pp. 60–74, 2012.
- [4] L. Badimon *et al.*, “C-reactive protein in atherothrombosis and angiogenesis,” *Frontiers in immunology*, vol. 9, p. 430, 2018.
- [5] A. P. Schroeder and E. Falk, “Vulnerable and dangerous coronary plaques,” *Atherosclerosis*, vol. 118, pp. S141–S149, 1995.
- [6] M. Navab *et al.*, “The yin and yang of oxidation in the development of the fatty streak: a review based on the 1994 George Lyman Duff memorial lecture,” *Arteriosclerosis, thrombosis, and vascular biology*, vol. 16, no. 7, pp. 831–842, 1996.
- [7] H. Nording, L. Baron, and H. F. Langer, “Platelets as therapeutic targets to prevent atherosclerosis,” *Atherosclerosis*, vol. 307, pp. 97–108, 2020.
- [8] R. S. Eshaq, “The effect of the local concentrations of nitric oxide and ADP on platelet adhesion and thrombus formation.” M.S Thesis, Louisiana Tech University, Ruston, LA, 2006.
- [9] A. P. Bye, A. J. Unsworth, and J. M. Gibbins, “Platelet signaling: a complex interplay between inhibitory and activatory networks,” *Journal of thrombosis and haemostasis*, vol. 14, no. 5, pp. 918–930, 2016.
- [10] F. Swieringa, H. M. H. Spronk, J. W. M. Heemskerk, and P. E. J. van der Meijden, “Integrating platelet and coagulation activation in fibrin clot formation,” *Research and practice in thrombosis and haemostasis*, vol. 2, no. 3, pp. 450–460, 2018.
- [11] J. M. Herbert, “Effects of ADP-receptor antagonism beyond traditional inhibition

- of platelet aggregation,” *Expert opinion on investigational drugs*, vol. 13, no. 5, pp. 457–460, 2004.
- [12] M. W. Radomski, D. D. Rees, A. Dutra, and S. Moncada, “S-nitroso-glutathione inhibits platelet activation in vitro and in vivo,” *British journal of pharmacology*, vol. 107, no. 3, p. 745, 1992.
- [13] R. S. Eshaq, K. Katie, K. Schipke, D. K. Mills, and stev, “Combined effect of ADP and nitric oxide on platelet adhesion,” *Houston society of biomedical engineering conference*. Houston, Texas, 2007.
- [14] R. S. Eshaq, C. Frilot, and S. A. Jones, “Comparison of l-arginine effects on platelet adhesion with and without flow,” *Biomedical Engineering Society Fall Annual Meeting*. Los Angeles, CA, 2007.
- [15] R. F. Furchgott and J. Zawadzki, “The obligatory role of endothelial cells in the relaxation of arterial smooth muscle by acetylcholine,” *Nature*, vol. 288, no. 5789, pp. 373–376, 1980.
- [16] J. E. Freedman, J. Loscalzo, M. R. Barnard, C. Alpert, J. F. Keaney, and A. D. Michelson, “Nitric oxide released from activated platelets inhibits platelet recruitment,” *The Journal of clinical investigation*, vol. 100, no. 2, pp. 350–356, 1997.
- [17] A. Radziwon-Balicka *et al.*, “Differential eNOS-signalling by platelet subpopulations regulates adhesion and aggregation,” *Cardiovascular research*, vol. 113, no. 14, pp. 1719–1731, 2017.
- [18] M. S. Crane, A. G. Rossi, and I. L. Megson, “A potential role for extracellular nitric oxide generation in cGMP-independent inhibition of human platelet aggregation: biochemical and pharmacological considerations,” *British journal of pharmacology*, vol. 144, no. 6, pp. 849–859, 2005.
- [19] D. J. Stuehr, N. S. Kwon, C. F. Nathan, O. W. Griffith, P. Feldman, and J. Wiseman, “N omega-hydroxy-L-arginine is an intermediate in the biosynthesis of nitric oxide from L-arginine,” *Journal of Biological Chemistry*, vol. 266, no. 10, pp. 6259–6263, 1991.
- [20] M. A. Marietta, “Nitric oxide synthase: function and mechanism,” in *Chemistry and Biology of Pteridines and Folates*, J. E. Ayling, M. G. Nair, and C. M. Baugh, Eds. Boston, MA: Springer, 1993, pp. 281–284.
- [21] L. J. McDonald and F. Murad, “Nitric oxide and cGMP signaling,” *Advances in pharmacology*, vol. 34, pp. 263–275, 1995.
- [22] E. Gkaliagkousi, J. Ritter, and A. Ferro, “Platelet-derived nitric oxide signaling and regulation,” *Circulation research*, vol. 101, no. 7, pp. 654–662, 2007.

- [23] R. C. Jin and J. Loscalzo, "Vascular nitric oxide: formation and function," *Journal of blood medicine*, vol. 1, p. 147, 2010.
- [24] U. Förstermann and W. C. Sessa, "Nitric oxide synthases: regulation and function," *European heart journal*, vol. 33, no. 7, pp. 829–837, 2012.
- [25] B. Li *et al.*, "Recent developments in pharmacological effect, mechanism and application prospect of diazeniumdiolates," *Frontiers in Pharmacology*, p. 923, 2020.
- [26] M. R. Miller and I. L. Megson, "Recent developments in nitric oxide donor drugs," *British journal of pharmacology*, vol. 151, no. 3, pp. 305–321, 2007.
- [27] L. J. Ignarro, C. Napoli, and J. Loscalzo, "Nitric oxide donors and cardiovascular agents modulating the bioactivity of nitric oxide: an overview," *Circulation research*, vol. 90, no. 1, pp. 21–28, 2002.
- [28] M. Y. Lee and S. L. Diamond, "A human platelet calcium calculator trained by pairwise agonist scanning," *PLoS computational biology*, vol. 11, no. 2, p. e1004118, 2015.
- [29] D. Varga-Szabo, A. Braun, and B. Nieswandt, "Calcium signaling in platelets," *Journal of Thrombosis and Haemostasis*, vol. 7, no. 7, pp. 1057–1066, 2009.
- [30] W. Bergmeier and L. Stefanini, "Novel molecules in calcium signaling in platelets," *Journal of thrombosis and Haemostasis*, vol. 7, pp. 187–190, 2009.
- [31] N. Wolska and M. Rozalski, "Blood platelet adenosine receptors as potential targets for anti-platelet therapy," *International Journal of Molecular Sciences*, vol. 20, no. 21, p. 5475, 2019.
- [32] W. E. Boden, S. K. Padala, K. P. Cabral, I. R. Buschmann, and M. S. Sidhu, "Role of short-acting nitroglycerin in the management of ischemic heart disease," *Drug Design, Development and Therapy*, vol. 9, p. 4793, 2015.
- [33] S. R. Sanakam, "Improved microchananel surfaces for the study of combined positive and negative feedback mechanisms in platelet adhesion." Ph.D. Dissertation, Louisiana Tech University, Ruston, LA, 2017.
- [34] R. R. Adams, "Positive and negative feedback effects of upstream thrombogenic regions on downstream platelet adhesion." Ph.D. Dissertation, Louisiana Tech University, Ruston, LA, 2017.
- [35] D. V Spiriyova, A. Y. Vorobev, V. V Klimontov, E. A. Koroleva, and A. E. Moskalensky, "Optical uncaging of ADP reveals the early calcium dynamics in single, freely moving platelets," *Biomedical optics express*, vol. 11, no. 6, pp. 3319–3330, 2020.

- [36] K. Takeuchi *et al.*, “Nitric oxide: inhibitory effects on endothelial cell calcium signaling, prostaglandin I₂ production and nitric oxide synthase expression,” *Cardiovascular research*, vol. 62, no. 1, pp. 194–201, 2004.
- [37] D. L. Bethesda, “Blood groups and red cell antigens,” *The Rh Blood Group. USA: National Center for Biotechnology Information*, pp. 1–6, 2005.
- [38] L. H. Grouse, G. H. Rao, D. J. Weiss, V. Perman, and J. G. White, “Surface-activated bovine platelets do not spread, they unfold,” *The American journal of pathology*, vol. 136, no. 2, p. 399, 1990.
- [39] J. W. Weisel and R. I. Litvinov, “Fibrin formation, structure and properties,” *Fibrous proteins: structures and mechanisms*, pp. 405–456, 2017.
- [40] M. H. Periyah, A. S. Halim, and A. Z. M. Saad, “Mechanism action of platelets and crucial blood coagulation pathways in hemostasis,” *International journal of hematology-oncology and stem cell research*, vol. 11, no. 4, p. 319, 2017.
- [41] M. Tomaiuolo, L. F. Brass, and T. J. Stalker, “Regulation of platelet activation and coagulation and its role in vascular injury and arterial thrombosis,” *Interventional cardiology clinics*, vol. 6, no. 1, p. 1, 2017.
- [42] F. Eisinger, J. Patzelt, and H. F. Langer, “The platelet response to tissue injury,” *Frontiers in medicine*, p. 317, 2018.
- [43] Z. Li, M. K. Delaney, K. A. O’Brien, and X. Du, “Signaling during platelet adhesion and activation,” *Arteriosclerosis, thrombosis, and vascular biology*, vol. 30, no. 12, pp. 2341–2349, 2010.
- [44] E. Falk and A. Fernández-Ortiz, “Role of thrombosis in atherosclerosis and its complications,” *The American journal of cardiology*, vol. 75, no. 6, pp. 5B–11B, 1995.
- [45] M. Y. Shen *et al.*, “Inhibitory mechanisms of resveratrol in platelet activation: pivotal roles of p38 MAPK and NO/cyclic GMP,” *British journal of haematology*, vol. 139, no. 3, pp. 475–485, 2007.
- [46] J. D. Beck, J. R. Elter, G. Heiss, D. Couper, S. M. Mauriello, and S. Offenbacher, “Relationship of periodontal disease to carotid artery intima-media wall thickness: the atherosclerosis risk in communities (ARIC) study,” *Arteriosclerosis, thrombosis, and vascular biology*, vol. 21, no. 11, pp. 1816–1822, 2001.
- [47] V. Fuster, B. Stein, J. A. Ambrose, L. Badimon, J. J. Badimon, and J. H. Chesebro, “Atherosclerotic plaque rupture and thrombosis. Evolving concepts,” *Circulation*, vol. 82, no. 3 Suppl, pp. II47–59, 1990.
- [48] A. I. MacIsaac and E. J. Topol, “Toward the quiescent coronary plaque,” *Journal of the American College of Cardiology*, vol. 22, no. 4, pp. 1228–1241, 1993.

- [49] Z. M. Ruggeri, "Platelets in atherothrombosis," *Nature medicine*, vol. 8, no. 11, pp. 1227–1234, 2002.
- [50] Z. M. Ruggeri and G. L. Mendolicchio, "Adhesion mechanisms in platelet function," *Circulation research*, vol. 100, no. 12, pp. 1673–1685, 2007.
- [51] B. Savage, E. Saldívar, and Z. M. Ruggeri, "Initiation of platelet adhesion by arrest onto fibrinogen or translocation on von Willebrand factor," *Cell*, vol. 84, no. 2, pp. 289–297, 1996.
- [52] J. F. Fullard, "The role of the platelet glycoprotein IIb/IIIa in thrombosis and haemostasis," *Current pharmaceutical design*, vol. 10, no. 14, pp. 1567–1576, 2004.
- [53] Z. M. Ruggeri, J. N. Orje, R. Habermann, A. B. Federici, and A. J. Reininger, "Activation-independent platelet adhesion and aggregation under elevated shear stress," *Blood*, vol. 108, no. 6, pp. 1903–1910, 2006.
- [54] M. H. Kroll, J. D. Hellums, L. V McIntire, A. I. Schafer, and J. L. Moake, "Platelets and shear stress," *Blood*, vol. 88, no. 5, pp. 1525–1541, 1996.
- [55] L. D. C. Casa, D. H. Deaton, and D. N. Ku, "Role of high shear rate in thrombosis," *Journal of vascular surgery*, vol. 61, no. 4, pp. 1068–1080, 2015.
- [56] X. Shi *et al.*, "Effects of different shear rates on the attachment and detachment of platelet thrombi," *Molecular Medicine Reports*, vol. 13, no. 3, pp. 2447–2456, 2016.
- [57] A. S. Kantak, B. K. Gale, Y. Lvov, and S. A. Jones, "Platelet function analyzer: Shear activation of platelets in microchannels," *Biomedical microdevices*, vol. 5, no. 3, pp. 207–215, 2003.
- [58] A. S. Kantak, B. K. Gale, Y. Lvov, and S. A. Jones, "Microfluidic platelet function analyzer for shear-induced platelet activation studies," in *2nd Annual International IEEE-EMBS Special Topic Conference on Microtechnologies in Medicine and Biology. Proceedings (Cat. No. 02EX578)*, 2002, pp. 169–173.
- [59] A. Kantak, Y. Lvov, D. K. Mills, J. G. Spaulding, and S. A. Jones, "Platelet function assessment in a microfabricated device," in *ASME International Mechanical Engineering Congress and Exposition*, 2002, vol. 36509, pp. 241–242.
- [60] R. S. Eshaq, K. Keeton, M. K. David, and S. A. Jones, "Paradoxical increased platelet adhesion with increased nitric oxide donor," *Biomedical engineering society annual fall meeting*. Chicago, IL, 2006.
- [61] M. G. Watson, J. M. Lopez, M. Paun, and S. A. Jones, "A novel dynamic layer-by-layer assembled nano-scale biointerface: functionality tests with platelet adhesion and aggregate morphology influenced by adenosine diphosphate," *Journal of*

thrombosis and thrombolysis, vol. 36, no. 4, pp. 448–457, 2013.

- [62] M. G. Watson, “Surface morphology of platelet adhesion influenced by activators, Inhibitors and Shear Stress.” Ph.D. Dissertation, Louisiana Tech University, Ruston, LA, 2010.
- [63] J. D. Tario Jr, K. A. Muirhead, D. Pan, M. E. Munson, and P. K. Wallace, “Tracking immune cell proliferation and cytotoxic potential using flow cytometry,” *Methods in molecular biology (Clifton, NJ)*, vol. 699, pp. 119–164, 2011.
- [64] C. R. Parish, “Fluorescent dyes for lymphocyte migration and proliferation studies,” *Immunology and cell biology*, vol. 77, no. 6, pp. 499–508, 1999.
- [65] G. A. Truskey, F. Yuan, and D. F. Katz, *Transport phenomena in biological systems*, vol. 2. Pearson, 2010.
- [66] A. Ramamurthi and R. S. Lewis, “Design of a novel apparatus to study nitric oxide (NO) inhibition of platelet adhesion,” *Annals of biomedical engineering*, vol. 26, no. 6, pp. 1036–1043, 1998.
- [67] F. Changyong, W. Hongyue, L. U. Naiji, C. Tian, H. E. Hua, and L. U. Ying, “Log-transformation and its implications for data analysis,” *Shanghai archives of psychiatry*, vol. 26, no. 2, p. 105, 2014.
- [68] P. Bellavite *et al.*, “A colorimetric method for the measurement of platelet adhesion in microtiter plates,” *Analytical biochemistry*, vol. 216, no. 2, pp. 444–450, 1994.
- [69] A. B. Van de Walle *et al.*, “The role of fibrinogen spacing and patch size on platelet adhesion under flow,” *Acta biomaterialia*, vol. 8, no. 11, pp. 4080–4091, 2012.
- [70] K. S. Sakariassen, L. Orning, and V. T. Turitto, “The impact of blood shear rate on arterial thrombus formation,” *Future science OA*, vol. 1, no. 4, p. FSO30, 2015.
- [71] S. Gogia and S. Neelamegham, “Role of fluid shear stress in regulating VWF structure, function and related blood disorders,” *Biorheology*, vol. 52, no. 5–6, pp. 319–335, 2015.
- [72] K. S. Sakariassen, “Thrombus formation on apex of arterial stenoses: the need for a fluid high shear stenosis diagnostic device,” *Future Cardiology*, vol. 3, no. 2, p. 193, 2007.
- [73] S. Xu, J. Piao, B. Lee, C. Lim, and S. Shin, “Platelet thrombus formation by upstream activation and downstream adhesion of platelets in a microfluidic system,” *Biosensors and Bioelectronics*, vol. 165, p. 112395, 2020.

- [74] S. M. Rahman and V. Hlady, "Microfluidic assay of antiplatelet agents for inhibition of shear-induced platelet adhesion and activation," *Lab on a Chip*, vol. 21, no. 1, pp. 174–183, 2021.
- [75] Y. N. Avtaeva, I. S. Mel'nikov, and Z. A. Gabbasov, "Real-time recording of platelet adhesion to fibrinogen-coated surface under flow conditions," *Bulletin of Experimental Biology and Medicine*, vol. 165, no. 1, pp. 157–160, 2018.
- [76] J. E. Freedman and J. Loscalzo, "Nitric oxide and its relationship to thrombotic disorders," *Journal of Thrombosis and Haemostasis*, vol. 1, no. 6, pp. 1183–1188, 2003.
- [77] C. Tziros and J. E. Freedman, "The many antithrombotic actions of nitric oxide," *Current drug targets*, vol. 7, no. 10, pp. 1243–1251, 2006.
- [78] J. E. Freedman, B. Ting, B. Hankin, J. Loscalzo, J. F. Keaney Jr, and J. A. Vita, "Impaired platelet production of nitric oxide predicts presence of acute coronary syndromes," *Circulation*, vol. 98, no. 15, pp. 1481–1486, 1998.
- [79] S. Sarkar and S. Kundu, "Structure and morphology of adsorbed protein (BSA) layer on hydrophilic silicon surface in presence of mono-, di-and tri-valent ions," *JCIS Open*, vol. 3, p. 100016, 2021.
- [80] C. I. Jones, "Platelet function and ageing," *Mammalian genome*, vol. 27, no. 7, pp. 358–366, 2016.
- [81] J. B. Segal and A. R. Moliterno, "Platelet counts differ by sex, ethnicity, and age in the United States," *Annals of epidemiology*, vol. 16, no. 2, pp. 123–130, 2006.